To the Graduate Council :

I am submitting herewith a thesis written by Vikram Krishnan entitled " A One Dimensional Model for the Thermal Response of a Decomposing Polymer". I have examined the final copy of this thesis for form and content and recommend that it be accepted in partial fulfillment of the requirements for the degree of Master of Science, with a major in Mechanical Engineering.

Majed Keyhani

M. Keyhani, Major Professor

We have read this thesis
and recommend its acceptance

Ron V. Arimilli

Accepted for the Council

Lew Minkel

Associate Vice Chancellor and
Dean of the The Graduate School

A ONE DIMENSIONAL MODEL FOR THE THERMAL RESPONSE OF A DECOMPOSING POLYMER

A Thesis

Presented for the

Master of Science

Degree

The University of Tennessee, Knoxville

Vikram Krishnan

August 1992

Acknowledgements

I express my sincere thanks to my Major Professor Dr. M. Keyhani. I am deeply indebted to him for his support and valuable guidance throughout the course of this research. He is the person who taught me to think like a engineer.

I also would like to thank Drs. Ke Nguyen and Rao Arimilli for their valuable suggestions and comments. I greatly appreciate the suggestions made by Rich Polehn during the course of this research.

The current project was sponsered by National Aeronautics and Space Administration under grant NAG8-862. I gratefully acknowledge its financial assistance for this research.

I am deeply indebted to my parents, brother and sister whose support, patience and untiring love are matchless.

ABSTRACT

A one dimensional transient model for the prediction of the temperature and pore pressure in a decomposing polymer with the capability of handling ablation at the surface is developed. The model is based on the conservation of mass, momentum and energy in a decomposing polymer. It was assumed that the pyrolysis gases and the solid are in local thermal equilibirium and therefore only one energy equation is needed for the conservation of energy. Various methods for the solution of the highly non linear pore pressure equation are outlined and one is proposed as appropriate. The effect of weakly coupled and fully coupled solution schemes as well as the use of nodelets scheme for the calculation of gas mass generation for the predicted temperature and pressure profiles are described. Although one energy equation is used, the limiting case of two energy equation, i.e., infinite and zero volumetric heat transfer coefficients between the gas and the solid is demonstrated. The effects of time stepping and effects of property variations on the in depth temperature and pressure profiles are also described. It is shown that use of sufficiently small time steps is important for the accurate prediction of the pressure and temperature profiles in the material. The effect of the Forcheimer term (inertial resistance) on the pressure solution is also shown. A numerical scheme for handling of surface recession is proposed. An algorithm for predicting the surface temperature for a chemically reacting boundary layer is suggested. Simulation of surface recession with linearly varying recession rate is also possible. The model is capable of handling multiple materials stacked one on top of the other.

CONTENTS

LIST OF FIGURES

LIST OF TABLES

LIST OF SYMBOLS

A	Area at the control volume face, m^2, ft^2
A_c	Area at node location, m^2, ft^2
A_j	Pre-exponential factor of the jth component, 1/s
B'_g	Non-dimensional gas mass flow rate (-)
B'_c	Non-dimensional char mass flow rate (-)
$\overline{D}$	Effective diffusion constant (-)
C_E	Ergun coefficient, function of porosity (-)
C_H	Stanton number for heat transfer (-)
C_M	Stanton number for mass transfer (-)
C_{pc}	Char specific heat, J/kg·K, Btu/lbm·R
C_{pv}	Virgin specific heat, J/kg·K, Btu/lbm·R
E_j	Activation energy of jth component, J/kgmole, Btu/lbm-mole
F	View factor (-)
h	Solid enthalpy, J/kg, Btu/lbm
h_c	Char material enthalpy, J/kg, Btu/lbm
h_v	Virgin material enthalpy, J/kg, Btu/lbm
h_{ew}	Enthalpy of edge gas evaluated at the wall temperature, J/kg, Btu/lbm
h_o	Enthalpy of formation, J/kg, Btu/lbm

h_g	Pyrolysis gas enthalpy, J/kg, Btu/lbm
h_{in}	Initial pyrolysis gas enthalpy, J/kg, Btu/lbm
h_t	Convective heat transfer coefficient , $J/m^2 \cdot s \cdot K$, $Btu/ft^2 \cdot s \cdot R$
h_w	Enthalpy evaluated at the wall temperature, J/kg, Btu/lbm
$h_i^{T_w}$	Enthalpy of component (i) of the boundary layer edge gas evaluated at wall temperature
H_r	Sensible enthalpy , J/kg, Btu/lbm
k	Bulk thermal conductivity, $J/m \cdot s \cdot K$, $Btu/ft \cdot s \cdot R$
K	Permeability, m^2, ft^2
Le	Lewis number, ratio of the thermal and mass diffusivities (-)
$\dot{m}_g$	Mass flow rate of the gas, kg/s, lbm/s
$\dot{m}_c$	Mass flow rate of the gas, kg/s, lbm/s
M	Pyrolysis gas molecular weight, kg/kgmole, lbm/lbmmole
n_j	Order of reaction of jth component, (-)
P	Gas pressure, Pa, lbm/ft^2
q_{bound}	Surface heat flux per unit area $J/m^2 \cdot s$, $Btu/ft^2 \cdot s$
q_{cond}	Surface heat flux due to conduction per unit area $J/m^2 \cdot s$, $Btu/ft^2 \cdot s$
q_{cons}	Constant heat flux input per unit area $J/m^2 \cdot s$, $Btu/ft^2 \cdot s$
q_{chem}	Surface heat flux due to chemical generation per unit area $J/m^2 \cdot s$
q_{sen}	Surface heat flux due to convection per unit area $J/m^2 \cdot s$, $Btu/ft^2 \cdot s$
q_{radin}	Surface heat flux due to radiation input per unit area $J/m^2 \cdot s$, $Btu/ft^2 \cdot s$

q_{radout}	Surface heat flux due to radiation output per unit area J/m ^{2}·s, Btu/ft ^{2}·s
q_{radout}	Surface heat flux due to diffusive fluxes per unit area J/m ^{2}·s, Btu/ft ^{2}·s
r_1	Instantaneous radius, m, ft
r_o	Original radius, m, ft
R	Universal gas constant, J/kgmole·K, Btu/lbmmole·R
Re	Reynolds number (-)
s	Surface recession rate, m/s, ft/s
t	Time, s
T	Temperature, K, R
T_{in}	Initial temperature, K, R
T_{cond}	Temperature for pure conduction, K, R
T_{dec}	Temperature due to phase change, K, R
T_{ave}	(T_{dec} + T)/2, K, R
T_{gas}	Ambient temperature, K, R
T_{ref}	Reference temperature for enthalpy of formation, K, R
T_w	Surface (Wall) temperature, K, R
u	Darcean velocity, m/s, ft/s
Z	Compressibility factor (-)
Z''_{iw}	Mass fractions of species at the wall, J/kg, Btu/lbm
Z''_{ie}	Mass fractions of the species at the edge of boundary layer, J/kg, Btu/lbm

Greek Symbols :

α	Absorbtivity of the material (-)
α_w	Absorbtivity of the material at the wall (-)
β	Degree of Char, (-)
ε	Emissivity of the material (-)
δT	(T_{dec} - T_{cond}), K, R
ΔT	(T_{dec} - T), K, R
ϕ	Porosity, (-)
γ	Coefficient of Forcheimer extension model, (-)
μ	Gas viscosity, kg/m·s, lbm/ft·s
ρ	Instantaneous bulk density of the solid, kg/m^3, lbm/ft^3
ρ_j	Instantaneous bulk density of the jth component, kg/m^3, lbm/ft^3
ρ_1	Instantaneous bulk density of the resin component (1), kg/m^3, lbm/ft^3
ρ_2	Instantaneous bulk density of the resin component (2), kg/m^3, lbm/ft^3
ρ_3	Instantaneous bulk density of the fiber component, kg/m^3, lbm/ft^3
ρ_c	Bulk char density, kg/m^3, lbm/ft^3
ρ_g	Pyrolysis gas density, kg/m^3, lbm/ft^3
ρ_v	Bulk virgin density, kg/m^3, lbm/ft^3
ρ_{cj}	Char density of the jth component, kg/m^3, lbm/ft^3
ρ_{vj}	Virgin density of the jth component, kg/m^3, lbm/ft^3
Γ	Resin volume fraction (-)

$\rho_e u_e C_M$ Mass transfer coefficient, kg/m ^{2}·s, lbm/ft ^{2}·s

$\rho_e u_e C_H$ Heat transfer coefficient, kg/m ^{2}·s, lbm/ft ^{2}·s

σ Stefan Boltzmann's constant, J/m ^{2}·s·K^4, Btu/ft ^{2}·s·R^4

Subscripts :

ℓ,cf Linearly interpolated value at the control volume face

cf Value at the control volume face

e Effective value

i Nodal position

Superscripts :

o Value at present time

CHAPTER 1

INTRODUCTION

During the firing of a solid propellant rocket motor the nozzle is subjected to severe environmental and oxidative conditions.The temperature of the hot gas can exceed 3000K and pressure can exceed 5 MPa. Since regenerative cooling is not available, solid propellant rocket motors depend heavily on ablative liner materials in order to survive such severe environment. The liner serves as a barrier between the high velocity, high temperature gas stream derived from the burning propellant and the metallic structure of the nozzle in order to maintain the structural integrity of the nozzle. A composite liner is light and possesses strength. Although the structural strength of the composite has been the primary task of many research groups, the thermal response of composite liners at high temperature is the focus of recent studies.

Composites which serve as ablative materials or sacrificial liners of rocket nozzles have a matrix of carbon fibers which are held in place with the help of a resin binder. The resin decomposes during the heating process. The problem can be thought of as a transient conduction process until the resin begins to decompose causing a phase change. This phase change leads to a production of pyrolysis gases which is partly stored in the pores created by this phase change, and the rest moves to adjacent regions, mostly in the direction of increasing permeability; i.e., the heated surface, and escape. The energy carried by the pyrolysis gases cools the solid in its path which is being heated by the incoming conduction heat transfer from the surface. Depending on the permeability of the decomposition and char zones, the stored gases in the pores may result in an excessive pressure build up in the material causing a phenomenon known as plylift. The pyrolysis zone moves inward in the material, leaving a charred region in its wake. Figure 1.1 illustrates the char, decomposing, and virgin zones in a thermally decomposing composite.

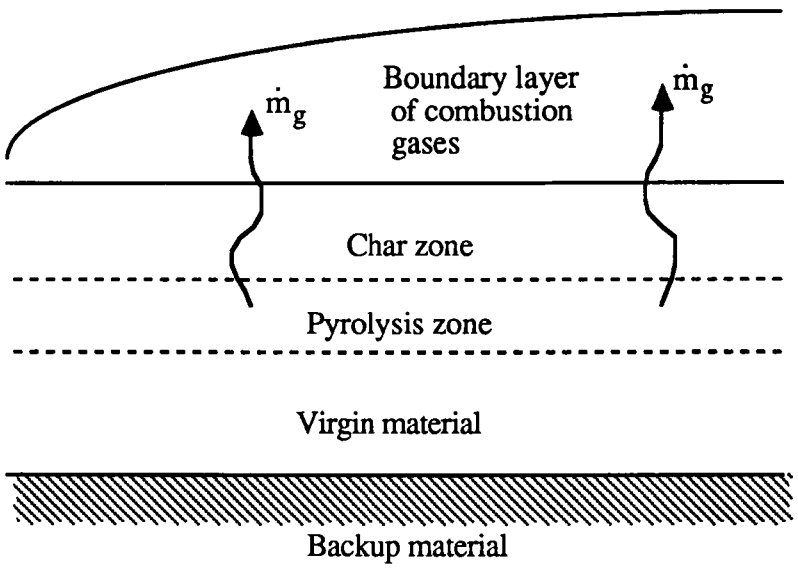

Fig. 1.1 Schematic of the physical model

1.1 Background

It seems that the origin of research in heat transfer and fluid flow in thermally decomposing solids lies in early work motivated by combustion of wood. A pioneering work in that area is due to Bamford et al. (1946), followed by many others such as Blackshear and Murty (1965), Tinney (1965), and Kung (1972). It all started with Bamford et al. when they subjected sheets of wood to various modes of heating and represented the thermal decomposition by a single exothermic reaction of the first order. Their main objective was to determine the rate at which fire develops in a given wooden structure from a given source. Later Kung in 1972 conducted a theoretical study to develop a mathematical model for wood burning. He also used a first order Arhenius rate equation for decomposition but used variable thermal conductivity, specific heat and density. The problem formulation led to a system of coupled non-linear parabolic differential equations which was solved using the traditional Crank-Nicholson method. He suggested that the effects of decomposition endothermicity, char conductivity and slab thickness have pronounced effect on the pyrolysis rate.

A closely related area of research (pore pressure prediction part of the problem) is work on transient compressible flow through porous media which is motivated by concerns on flow in underground porous formations. Numerous papers have been published in this area, among them are articles by Bruce et al. (1953). Bruce et al. developed a numerical procedure for solving the unsteady equation for the production of gas in linear and radial systems solving for the pressure distribution. This is of great importance in natural gas and oil reservoirs. Beavers and Sparrow (1971) studied the effects of high Reynolds number flow in porous materials when inertial resistances become high. Later Morrison (1972) analytically investigated the transient flow of an ideal gas in a porous cylinder. He used two models to describe the flow, one being the isothermal and the other adiabatic.

There is a large body of literature on thermally degrading polymers dating back to early 1960's (mostly as technical reports). These early efforts were concerned with thermal response of charring ablator heat shields subjected to aerodynamic heating (reentry problem). During the last fifteen years research activity in this area has increased, this time motivated by the concerns for protection of solid rocket motor nozzles. Henderson and co-workers have published several papers in this area, some of which were focused on one-dimensional modeling of this phenomenon (Henderson et al., 1985, 1987 and 1988). The first citation (1985) reported a model with one energy equation with no pore pressure build up; i. e., the decomposition gases were assumed to leave the material as soon as generated. Henderson and Wiecek (1987,1988) improved the earlier model by adding a momentum equation based on the Darcy law, and included the thermal expansion effect . They reported that the adjacent nodal values of the transport properties, thermal conductivity, permeability and viscosity were used to calculate their respective harmonic mean values at the control volume interfaces. Recently Florio and Henderson (1991) removed the assumption of local-thermal equilibrium between the solid and the decomposition gases in

the earlier model by using two energy equations. Also, the Forcheimer term was added to the momentum equation to account for the microscopic inertial effect.

Among other relevant previous studies the works of Maruyama et al. (1991), and Sullivan and Salamon (1990) are cited. The work of Maruyama et al. did not involve decomposition phenomenon, however, their study included the effect of radiation heat transfer within the porous material. A rigorous study of thermal response of a charring-decomposing polymer may require the consideration of radiation heat transfer at the pore level. The work of Sullivan and Salamon is important since it has a unified approach to the fully coupled solution of the thermal field, flow field and the stress field.

1.2 Objectives of the Present Study

It may seem that as far as one dimensional modeling is concerned the work of Henderson and co-authors should be sufficient, and further research should focus on two-dimensional modeling of the problem. That observation may have been true if the problem did not involve highly variable thermophysical properties, however, that is not the case. Therefore, the details of computational procedures for evaluation of thermophysical properties play a major role in the accuracy of the predictions, and deserve careful consideration. A specific area of concern has been the accuracy of pore pressure prediction. This is due to the fact that existing models are predicting very high pore pressures that seem unrealistic. The main property affecting the pore pressure prediction is the permeability of the material, which for some carbon phenolic composites may increase by seven orders of magnitude from the virgin state to fully charred condition.

Many researchers in this area have not considered various aspects and details involved in the numerical modeling of this phenomenon. The coupling of the mass conservation, momentum and the gas law leads to a highly non-linear equation for pore pressure. The various methods in which the properties in the pressure equation can be

evaluated are demonstrated. Moreover, the maximum effect of use of two energy equations, i.e., infinite and zero volumetric heat transfer coefficients between the gas and solid, is demonstrated. This is accomplished via nullifying the advected energy term in the computational domain. The details covered in this study include the effect of fully or weakly coupling of the governing equations, and the effect of various procedures for evaluation of the decomposition gas generation, and the effective conductance for gas flow.

The main contribution of this study is to introduce the various schemes for calculation of the effective conductance for flow of the decomposition gases, which yield vastly different pore pressure predictions. A scheme, named the modified harmonic mean, is introduced to take into account the highly non-linear behavior of the permeability in the pressure equation.

The importance of surface ablation is derived from the fact that as the material is removed from the nozzle surface, the rocket will be operating with a larger radius thus reducing the effective thrust. This could cause a severe decline in the performance of the rocket motor. An efficient numerical scheme for prediction of the surface recession is proposed.

CHAPTER 2

THERMAL MODEL

As stated earlier this model is based on transient one-dimensional conservation equations for mass, momentum, and energy along with equation of state for pyrolysis gases, and nth order kinetic rate equations (Arrhenius decomposition) describing the rate of production of gases. The governing equations are based on the following assumptions.

i) Local thermal equilibrium exists between the fluid and the solid.

ii) Decomposition gases are modeled as a single gas which obeys the gas law

iii) Decomposition gases are non-reactive.

iv) The fluid motion is governed by Darcy-Forcheimer equation.

v) Thermal radiation at the pore level is neglected.

2.1 Decomposition

The nth order Arhenius decomposition of the material components is described by

$$\frac{\partial \rho_j}{\partial t} = -A_j e^{-\frac{E_j}{RT}} \rho_{vj} \left(\frac{\rho_j - \rho_{cj}}{\rho_{vj}} \right)^{n_j} \qquad (2.1)$$

Due to the non availibility of specific data for numerous components in a polymer, only 3 important constituents are considered. This rate equation could be extended to n components, each of them undergoing decomposition with different rate constants. For most Carbon Phenolic type compounds, the material density can be broken up into three components, two of the components comprise the resin portion and the third component being the carbon fiber. The resin and the fiber component could decompose. The overall

density of the carbon phenolic would then be

$$\rho = \Gamma\left(\rho_1 + \rho_2\right) + \left(1 - \Gamma\right)\rho_3 \qquad (2.2)$$

where Γ is the resin fraction.

2.2 Mass Conservation Equation

Consider a control volume having a porosity of ϕ and the gas flow designated as $\dot{m}_g$. The amount of gas generated will be equal to the rate of the change in the density of the solid material. Using the conservation of mass with the proper coordinate directions one obtains

$$\frac{\partial}{\partial t}\left(\phi \rho_g A_c\right) + \frac{\partial \dot{m}_g}{\partial x} = - A_c \frac{\partial \rho}{\partial t} \qquad (2.3)$$

where the gas density in the storage term is calculated by the gas law,

$$\rho_g = \frac{P M}{Z R T} \qquad (2.4)$$

where the first term in Eq. (2.3) represents the rate of storage of gas in the control volume, second term the net gas flow into the control volume and the third term represents the amount of gas generated due to decomposition. The amount of gas generated is obtained using the Arhenius rate equation.

2.3 Energy Conservation Equation

The mathematical representation of the first law of thermodynamics to a control volume is

$$\frac{\partial}{\partial t}\left(\rho h A_c\right) + \frac{\partial}{\partial x}\left(\dot{m}_g h_g\right) = \frac{\partial}{\partial x}\left(kA \frac{\partial T}{\partial x}\right) \qquad (2.5)$$

The first term represents the rate of storage of energy in the control volume, the second term represents the net energy due to gas advection and the third term shows the energy change due to conduction. It is convenient to imagine that partially pyrolyzed material may be regarded as a mixture of pure char and pure plastic. The total energy content per unit volume can thus be written as the mass weighted average of the energy due to char, plastic and gas components.

$$\rho h = \beta \rho_c h_c + (1 - \beta)\rho_v h_v + \phi \rho_g h_g \tag{2.6}$$

where β is given by $$\beta(t) = \frac{\rho_v - \rho}{\rho_v - \rho_c} \tag{2.7}$$

The last term in Eq. (2.6) accounts for the storage of gas in the pores of the control volume. By differentiating the storage term of the energy equation with respect to time one obtains

$$\frac{\partial}{\partial t}(\rho h A_c) = A_c\left[\overline{\rho C_p}\frac{\partial T}{\partial t} + \bar{h}\frac{\partial \rho}{\partial t} + h_g \frac{\partial}{\partial t}(\phi \rho_g)\right] \tag{2.8}$$

where

$$\bar{h} = \frac{\rho_v h_v - \rho_c h_c}{\rho_v - \rho_c} \tag{2.9}$$

$$\overline{\rho C_p} = \beta \rho_c \overline{C_{pc}} + (1 - \beta)\rho_v \overline{C_{pv}} + \phi \rho_g \overline{C_{pg}} \tag{2.10}$$

$$\overline{C_p} = \frac{\int_{T^o}^{T} C_p \, dT}{T - T^o} \tag{2.11}$$

The initial condition specific enthalpies were calculated by

$$h_{in} = h_o + \int_{T_{ref}}^{T_{in}} C_p \, dT \qquad (2.12)$$

In order to represent the final energy equation in terms of temperature, the future values of the specific enthalpies of char component, virgin component, and decomposition gas were represented by

$$h = h^o + \overline{C_p}\left(T - T^o\right) \qquad (2.13)$$

By combining the mass conservation and the energy conservation equation and expanding the convection term and grouping the appropriate terms which make physical sense one obtains

$$A_c \overline{\rho C_p} \frac{\partial T}{\partial t} + \dot{m}_g \frac{\partial}{\partial x}\left(\overline{C_{pg}} T\right) = \frac{\partial}{\partial x}\left(kA \frac{\partial T}{\partial x}\right) +$$

$$A_c \left(h_g - \bar{h}\right) \frac{\partial \rho}{\partial t} + \dot{m}_g \frac{\partial}{\partial x}\left[\left(\overline{C_{pg}} T^o - h_g^o\right)\right] \qquad (2.14)$$

The terms in the resulting expression represent sensible energy accumulation, net advected energy, net conduction, phase change energy due to decomposition and the variable property effect due to advection. The phase change energy term is modelled as a source term, and implicit representation is acheived via iteration.

2.4 Pressure Equation

The momentum equation describing the flow of fluids in porous media is given by

the Darcy - Forcheimer relation. For a one dimensional flow through a porous structure, the apparent velocity of a fluid flowing through the porous bed is defined by the volume rate per unit area normal to the direction of the flow.

$$-\frac{\partial P}{\partial x} = \frac{\mu}{K} u + \frac{C_E}{\sqrt{K}} \rho_g |u| u \tag{2.15}$$

Equation (2.15) can be written as

$$u = -\frac{K}{\mu\gamma} \frac{\partial P}{\partial x} \tag{2.16}$$

where

$$\gamma = \left[1 + C_E \, Re\right] \tag{2.17}$$

and

$$Re = \frac{\sqrt{K} \, \rho_g |u|}{\mu} \tag{2.18}$$

where K is the permeability, μ the viscosity and P the fluid pressure. Because of the highly tortuous paths followed by the fluid elements, microscopic inertial effects become significant, and the relation between velocity and pore pressure becomes nonlinear. Forcheimer(1901) proposed that the Darcy's law be modified by an inclusion of a second order term in velocity(γ>1). It has been shown that for high Reynolds number the Darcy-Forcheimer model agrees well with the experimental results carried out by Burke and Plummer(1928), Ergun and Orning (1949), Green and Duwez(1951) and Ergun(1952). Further generalization was proposed by Polubarinova-Kochina(1962) which includes the local acceleration term. Later Beavers and Sparrow(1971) proposed the inclusion of the convective acceleration term. In the present study the macroscopic inertial and macroscopic viscous effects are neglected since the microscopic effects are the dominant factors in this

case.

Coupling the momentum equation, conservation of mass and the ideal gas law one obtains a highly non-linear equation for the pressure in the pores of a porous material.

$$\frac{\partial}{\partial t}\left(\frac{\phi M A_c}{Z R T} P\right) = \frac{\partial}{\partial x}\left[\left(\frac{K}{\mu\gamma}\right)_e \left(\rho_g\right)_e A \frac{\partial P}{\partial x}\right] - A_c \frac{\partial \rho}{\partial t} \quad (2.19)$$

The time accurate solution of the pore pressure equation and the energy equation, subjected to recession at the surface due to a varying heat flux at the boundary is the main task of the present work. The highly nonlinear nature of the pressure equation along with the fact that the permeability of the material changes by several orders of magnitude are the key reasons for focussing on procedures for evaluation of properties used in that equation. The compact form of the Darcy Forcheimer model for the flow of gas in a porous structure (Eq. 2.16) is similar to the Fourier's law of conduction heat transfer. Therefore as far as the gas velocity is concerned one needs a model for evaluation of effective conductance for the flow as well as the gas density to be used in the computation of the mass flow rate crossing each face of the control volume.

CHAPTER 3

SURFACE BOUNDARY CONDITION

The boundary conditions and/or the initial condition are the driving forces for any problem in nature. The surface boundary condition for the present model may be in two forms.

3.2 General Boundary Condition

This type of boundary condition may include convection, radiation and constant heat flux components. The constant temperature condition can also be obtained as a special case of convective heat transfer by setting the convective heat transfer coefficient to infinity and the ambient gas temperature set equal to the constant value for the boundary as required.

$$q_{bound} = h_t\left(T_w - T_{gas}\right) + \varepsilon\sigma\left(T_w^4 - T_{gas}^4\right) + q_{const} \qquad (3.1)$$

3.3 Chemically Reacting Boundary Layer

In reality the rocket nozzle liner is subjected to a chemically reacting boundary layer caused by the flow of hot combustion gases. The reacting boundary layer over the surface reacts with the surface and an exchange of enthalpy fluxes take place. A schematic of the various types of fluxes entering and leaving the boundary control volume is shown in Fig 3.1. Energy fluxes leaving the boundary control volume include conduction into the material, radiation away from the surface, energy flux out due to condensed phase material such as liquid run off, and gross blowing at the surface. Energy flux input to the surface include radiation in from the boundary layer and enthalpy fluxes

due to char and pyrolysis gas flow rates. All the diffusive fluxes and convected fluxes fom the gas boundary layer are represented by q_{diff}.

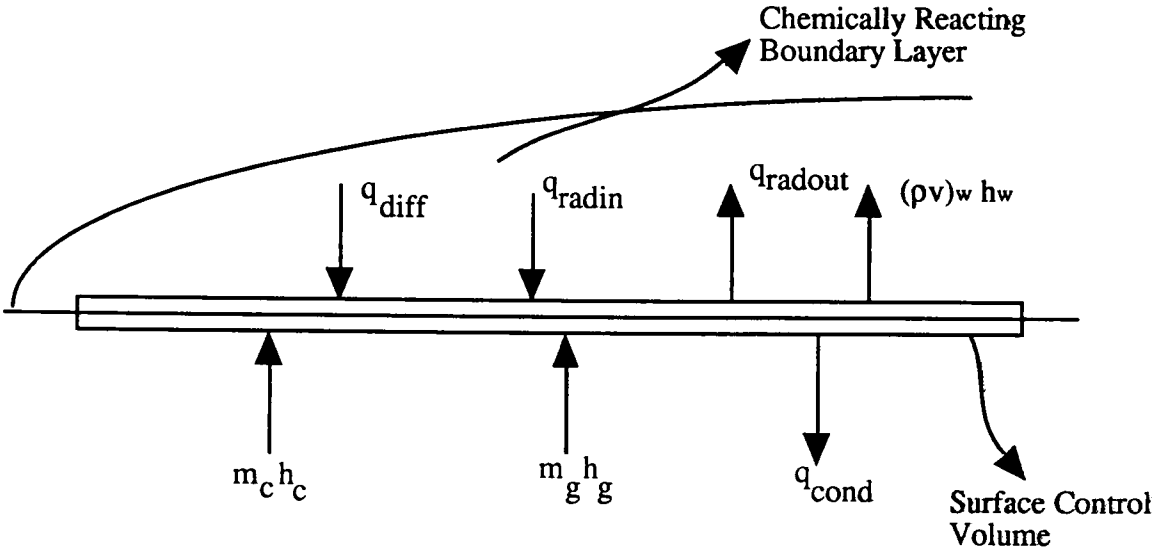

Fig. 3.1 Chemically reacting boundary layer

Performing an energy balance at the surface would yield

$$q_{diff} + q_{radin} + \dot{m}_c h_c + \dot{m}_g h_g - q_{radout} - (\rho v)_w h_w - q_{cond} = 0 \qquad (3.2)$$

where

$$(\rho v)_w = (\dot{m}_c + \dot{m}_g) \qquad (3.3)$$

The details involved in the development of the chemically reacting boundary layer equations are not the subject of this work. One can use the film coefficient model for solving the boundary layer in contact with an ablating surface. The Boundary Layer Integral Matrix Procedure (BLIMP) is yet another method of solving a reacting boundary layer. The BLIMP solution is accurate but time consuming. The film coefficient model is an efficient scheme for handling the reacting boundary layer. The film coefficient model

is based on the fact that there is char injection to the surface. The film coefficient model is thus able to solve for char injection which in turn would predict surface recession rate. The film coefficient model gives an expression for the diffusive transport rates of mass and energy through the boundary layer wall.

The diffusive fluxes from the boundary layer to the wall for equal diffusion coefficients can be written as [7].

$$q_{diff} = \rho_e u_e C_M \left[\sum_i \left(Z''_{ie} - Z''_{iw} \right) h_i^{T_w} \right] + \rho_e u_e C_H \left(H_r - h_{ew} \right) \tag{3.4}$$

The overall surface energy balance balance Eq.(3.2), can be written as

$$\rho_e u_e C_H \left(H_r - h_{ew} \right) + \rho_e u_e C_M \left[\sum_i \left(Z''_{ie} - Z''_{iw} \right) h_i^{T_w} \right] +$$

$$(\dot{m}_c h_c + \dot{m}_g h_g) - (\dot{m}_c + \dot{m}_g) h_w + \alpha_w q_{radin}$$

$$- F \sigma \varepsilon_w T_w^4 - q_{cond} = 0 \tag{3.5}$$

where

$\rho_e u_e C_H \left(H_r - h_{ew} \right)$ = Convective heat flux

$\rho_e u_e C_M \left[\sum_i \left(Z''_{ie} - Z''_{iw} \right) h_i^{T_w} \right]$ = Chemical reaction heat flux

$(\dot{m}_c h_c + \dot{m}_g h_g) - (\dot{m}_c + \dot{m}_g) h_w$ = Net heat flux due to bulk flow

$\alpha_w q_{rad}$ = Absorbed radiant heat flux

$F \sigma \varepsilon_w T_w^4$ = Emitted radiant heat flux

q_{cond} = In-depth conduction heat flux

The net boundary heat flux into the material should equal to the in-depth conduction heat transfer. Rearranging terms and solving for boundary heat flux q_{bound} we have

$$q_{bound} = q_{cond} = \rho_e u_e C_H \left(H_r - h_{ew}\right) + \rho_e u_e C_M \left[\sum_i \left(Z''_{ie} - Z''_{iw}\right) h_i^{T_w}\right]$$
$$(\dot{m}_c h_c + \dot{m}_g h_g) - (\dot{m}_c + \dot{m}_g) h_w + \alpha_w q_{radin} - F\sigma\varepsilon_w T_w^4 \qquad (3.6)$$

The above energy balance is valid only for frozen boundary layer with a reactive wall.

The present model requires that C_M/C_H be input as a constant. The value of this constant is a measure of the ratio of the mean mass transfer aspects of the boundary layer to the mean heat transfer. The present program also allows for the <u>blowing correction</u>. The value of C_H depends partly on $\dot{m}_g$. If we denote the C_H with $\dot{m}_g = 0$ as C_{Ho}, then the corrected C_H is represented by [20]

$$C_H/C_{Ho} = (e^{\varepsilon} - 1)/\varepsilon \qquad (3.7)$$

where $\varepsilon = (2 * B'^* \lambda)$ and $(B' = B'_g + B'_c)$

For laminar flow $\lambda = 0.5$, but for turbulent flow $\lambda = 0.4$ correlates data slightly better.

The <u>radius ratio correction</u> is yet another correction introduced to modify the heat transfer coefficient $\rho_e u_e C_H$. It is given by

$$C_H/C_{Ho} = (r_1/r_o)^{\left(\frac{1.8 - 2n}{1 - n}\right)} \qquad (3.8)$$

where n is called the burning rate exponent.

The term q_{sen} represents the sensible convective heat flux. Physically this is a convective heat flux which would occur for a frozen boundary layer and a non catalytic wall in the absence of mass transfer. It does not include chemical energy contributions. The q_{sen} can be written as

$$q_{sen} = \rho_e u_e C_H \left(H_r - h_{ew} \right) \qquad (3.9)$$

where H_r is the recovery enthalpy which is input by the user.

The heat transfer coefficient $\rho_e u_e C_H$ and the recovery enthalpy are time dependent variables input by the program user in the form of time dependent tables. The present model does have the capability to have time dependent thermochemistry tables. The h_{ew} is a part of the edge gas tables. The term q_{chem} represents the net of a number of fluxes of chemical energies at the surface. The Z" difference term represents transport of chemical energies associated with chemical reactions at the wall and in the boundary layer, it is the chemical energy parallel to the sensible convective heat flux term. The Z" driving forces for diffusive mass transfer include effects of unequal diffusion coefficients. For equal diffusion coefficients the Z" difference reduces to the mass fractions. The $\dot{m}_c h_c$ and $\dot{m}_g h_g$ terms represent energy fluxes arriving at the surface from within the solid material and the $(\dot{m}_c + \dot{m}_g) h_w$ term represents the energy leaving the surface in the gross motion(blowing) of the gas adjacent to the surface. The quantity B'g is given by $B'g = \dot{m}_g / \rho_e u_e C_M$. The pyrolysis gas enthalpy is obtained from the input temperature and pressure dependent temperature/enthalpy table. The quantities T_w, Z" and h_w are input by the user in a table with pressure and temperature as independent variables.

The present model requires a thermochemistry table similar to the output generated by the ACE code called the B' tables. The B' tables contain the revelant data

for forming the surface energy balance. A brief desription and physical analogies of the terms in the surface energy balance is provided.

3.3 Surface Heat Flux Data

The input tables are the edgegas table, the surface thermochemistry table and the time dependent boundary tables. The whole concept of a boundary layer over the surface can be viewed as a case of a variable flux input to the surface. Therefore using the thermochemistry, edgegas and time dependent tables the present code generates a set of heat flux tables which has dependent variables T_w, B'_g and B'_c. B'_g and B'_c are dimensionless gas mass flow and char injection rates to the surface. They are normalized via $\rho_e u_e C_M$. Sample edgegas and surface thermochemistry data are shown below.

Sample edgegas data

P (atm)	B'_g	B'_c	T_w	$\overline{D}$	$\sum Z''_{ie} h_i^{T_w}$	h_{edge}
34.23	0.0	0.0	7200	0.667	3015.0	1492.6
34.23	0.0	0.0	6300	0.667	2382.9	1044.1
'	'	'	'	'	'	'
'	'	'	'	'	'	'

Sample surface data

P (atm)	B'_g	B'_c	T_w	$\overline{D}$	$\sum Z''_{iw} h_i^{T_w}$	h_{wall}
34.23	0.5	0.5	6168.4	0.667	4978.9	3398.2
34.23	0.5	0.2	5494.4	0.667	3233.7	1799.2
'	'	'	'	'	'	'
'	'	'	'	'	'	'

Surface heat flux data are formed prior to marching in time. The surface heat flux data have the following columns in its output. For each B'_g , the following values are tabulated :

B'c, total surface heat flux and its components namely, heat flux due to chemical energy, heat flux due to convection, input radiation flux and radiant heat flux out. A sample surface heat flux data is shown below. Figures 3.2 and 3.3 give a graphical presentation of the surface heat flux boundary condition and the surface recession rate as a function of surface temperature with B'_g as a parameter.

Sample surface heat flux data

$B'_g = 0.5$

Temp	B'_c	q_{bound}	q_{sen}	q_{chem}	q_{radin}	q_{radout}
900.0	0.001	3980.2	1969.15	1458.5	552.81	0.265
4500.0	0.09	1209.7	739.8	83.06	552.81	165.9

$B'_g = 0.2$

Temp	B'_c	q_{bound}	q_{sen}	q_{chem}	q_{radin}	q_{radout}
900.0	0.001	3884.1	2112.2	1219.27	552.81	0.265
4500.0	0.100	1218.8	788.7	43.23	552.81	165.911

The boundary equation is an approximation and its usefulness depends on the transfer coefficient approach. For most heat and mass transfer problems the transfer coefficient approach has successfully correlated both data and exact solution for unity (or near unity) Lewis number. Equation (3.5) attempts to extend the transfer coefficient approach to both non-unity Lewis number and unequal diffusion coeficient problems, although allowing for net mass transfer and chemical reaction effects. The solution of the boundary energy balance yields B'c , the non-dimensional amount of char injected to the surface, which in turn is used to calculate the surface recession.

$$\dot{s} = \frac{\dot{m}_c}{\rho} \qquad (3.10)$$

where ρ is the instantaneous density of the solid at the surface.

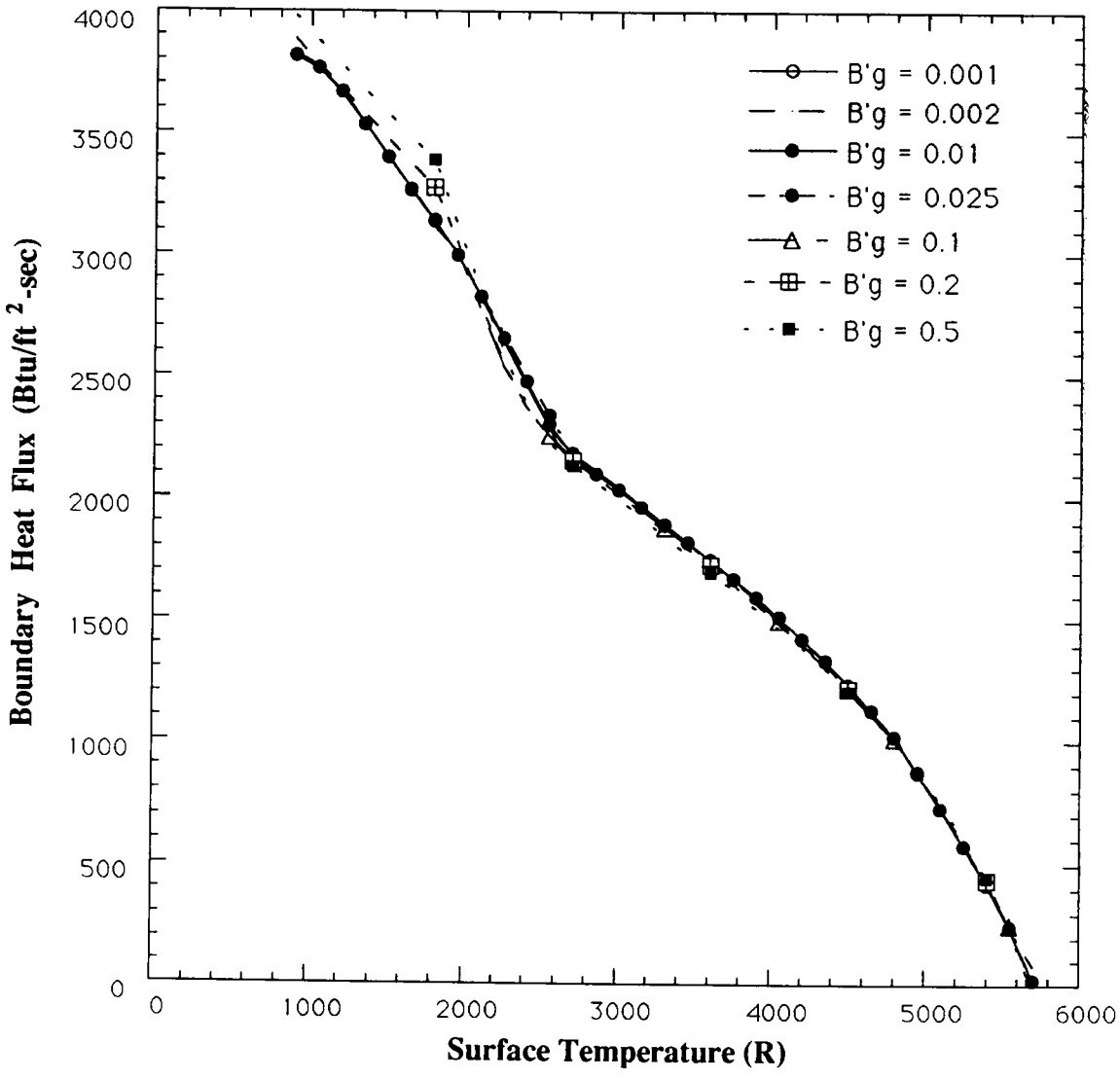

Fig. 3.2 Plot of heat flux versus temperature for various B'g

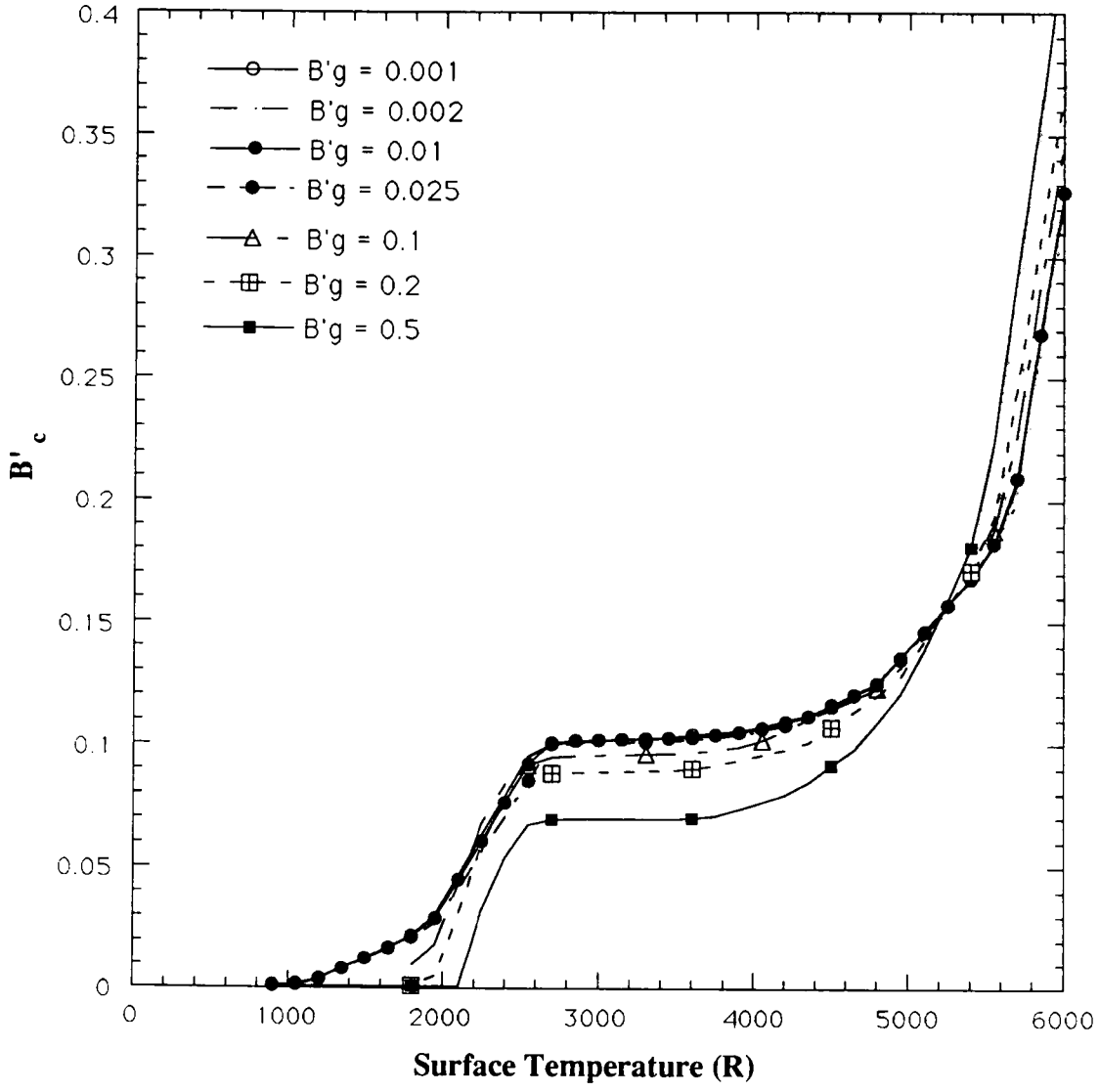

Fig 3.3 Plot of B'c versus temperature for various B'g

CHAPTER 4

SOLUTION PROCEDURE

The control volume technique proposed by Patankar(1980) was used to solve the system of governing equations. A generic control volume for space is shown in the figure below

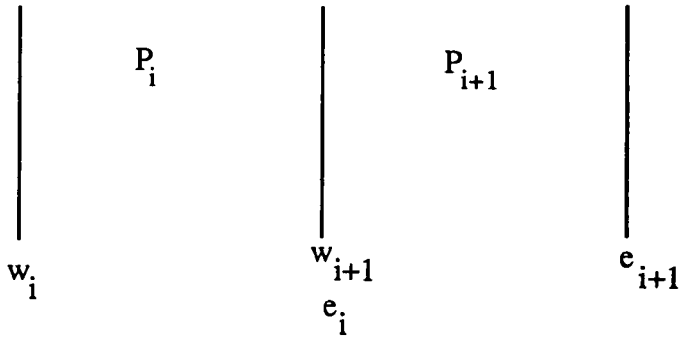

Fig 4.1 Generic control volume

The node is located at point P which lies in the center of the control volume, (e) represents the east face boundary and (w) represents the west face boundary. The governing equations were integrated from the west face to the east face in space , and from time t to t + dt.

Using the staggered approach normally used for coupled convection and diffusion problems, the extensive (temperature , pressure) variables lie in the centers of the control volumes and the intensive variables (velocity, mass flow rate) are staggered, that is they lie at the faces of the control volumes. Figure 4.2 shows a typical control volume of an extensive and intensive variable.

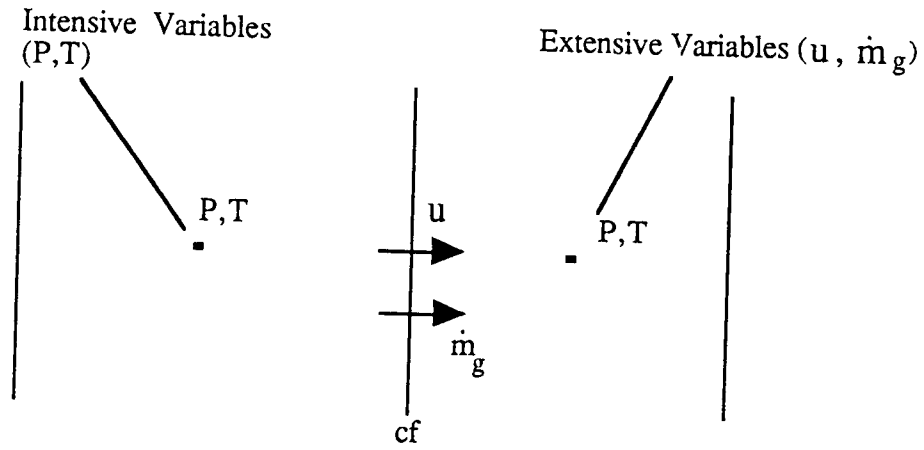

Fig 4.2 Typical variables in a control volume

The integration of the governing equations is similar to a finite differencing and results in a set of algebraic equations which have to be solved till convergence. Central differencing scheme is used in modelling of the advection term in the energy equation. Since the energy transport is diffusion dominated, the resulting algebraic equations satisfy the basic criteria for a stable solution. The scheme used is fully implicit in temperature hence does not possess a restriction on time step. A brief dicussion of each of the components of the model is provided and methods by which they are evaluated.

4.1 Decomposition

The decomposition of the material is assumed to obey the Arhenius rate equation. The nth order Arhenius rate equation can be written as

$$\frac{\partial \rho_j}{\partial t} = -A_j e^{-\frac{E_j}{RT}} \rho_{vj} \left(\frac{\rho_j - \rho_{cj}}{\rho_{vj}} \right)^{n_j} \qquad (4.1)$$

It is to be noted that the decomposition depends upon density and temperature which may also vary with time. If the temperature and density variations during a time

interval are large to significantly affect the decomposition rate, either a small time step must be used or a temperature and density more representative of the average time interval should be employed in order to obtain a stable solution. Generally a node undergoing decomposition experiences a density decrease and temperature increase. The above equation suggests that using the density at the beginning of the time step will overpredict the decomposition rate while using the temperature at the beginning of the time step will underpredict the decomposition rate. These numerical errors are usually associated with a too large or too small value of time step, and it is therefore appropriate to consider an implicit treatment of density while treating the temperature in an explicit manner. An explicit treatment of the temperature is possible because the decomposition energy of the organic constituents is small and as such, the coupling between the energy and mass conservations is weak for nodes in the decomposition region. An effective "implicit" treatment of density can be obtained by integration of the above expression holding the temperature constant.

The integration of the Arhenius rate expression results in the following

$$\frac{d\rho}{dt} = \frac{\rho_{ci} - \rho^o + \left[\left(\rho^o - \rho_{ci} \right)^{1-n_i} - \left(\frac{1 - n_i}{n_i - 1} \right) A\, e^{-\frac{E}{RT}} \Delta t \right]^{\frac{1}{(1-n_i)}}}{\Delta t} \qquad (4.2)$$

when n = 1 then

$$\frac{d\rho}{dt} = \left(\frac{\rho^o - \rho_{ci}}{\Delta t} \right) \left[e^{-K e^{-\frac{E}{RT}} \Delta t} - 1 \right] \qquad (4.3)$$

The implicit relations yield a much more stable solution than that obtained by treating density explicitly.

4.2 Nodelet Concept

For most problems involving decomposition of a material, it has been observed that a finer definition is required for an accurate calculation of the decomposition than that for energy conservation. As a result the control volume for evaluation of the decomposition is finer than that required for solving the energy equation. Therefore space derivatives for energy equation is based on nodes whereas for decomposition are based on a system of nodelets within each node. Figure 4.3 shows a typical node and the nodelets associated with the node.

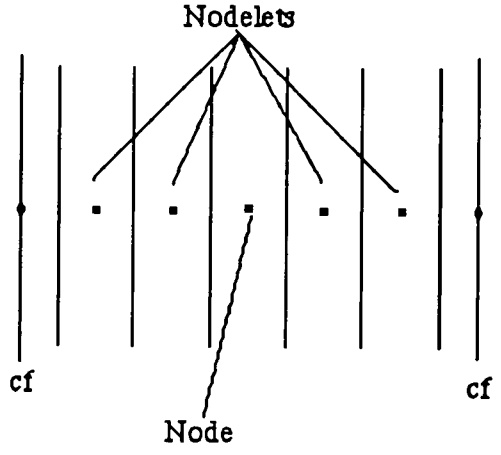

Fig 4.3 Nodelets for a typical control volume

The exact density is thus evaluated at each nodelet using Eq 4.2. The nodelet temperature is determined by linear interpolation of the temperatures at neighbouring control volumes. In the present model the nodelets are equally spaced and equal numbers of nodelets are placed to west and east of the node. The number of nodelet is an input value and should be an odd number. The total nodal density change is evaluated as the weighted average of the density change of the individual nodelets.

4.3 Description of Properties

i) **Specific heat** : Following the definition of enthalpy, the specific heat of virgin, char and gas could be determined by integrating the expression described by Eq. (2.11). In this model, partially degraded material is thought of as mixture of pure char and pure virgin. The specific heat of partially pyrolysed material is thus a mass weighted average of the virgin and char specific heats as described by Eq. (2.10).

The initial condition specific enthalpies were calculated by Eq (3.12)

$$h_{in} = h_o + \int_{T_{ref}}^{T_{in}} C_p \, dT \qquad (4.1)$$

In order to represent the final energy equation in terms of temperature, the future values of the specific enthalpies of char component, virgin component, and decomposition gas were represented by Eq (2.13)

$$h = h^o + \overline{C_p}\left(T - T^o\right) \qquad (4.2)$$

ii) **Thermal conductivity** : The treatment of thermal conductivity for partially degraded material is an interesting subject. In the present model the thermal conductivity is evaluated as a linear interpolation of the virgin material mass fraction,

$$K = x K_v + \left(1 - x\right) K_c \qquad (4.3)$$

where the partially degraded material is regarded as a mixture of virgin material and

pure char. The quantity 'x' is defined as the mass fraction of pure virgin material in the mixture,

$$x = \frac{\rho_v}{\rho_v - \rho_c}\left(1 - \frac{\rho_c}{\rho(t)}\right) \qquad (4.4)$$

However, theory shows that for decomposing materials, as soon as decomposition begins many materials display a conductivity appreciably lower than either virgin conductivity or char conductivity. This could not be handled by the above expression.

iii) **Pyrolysis gas enthalpy** : The final governing equation for energy shows that the pyrolysis gas enthalpy play an important part in the source term and contributes both to the chemical generation as well as the net convection of the pyrolysis gases. It is to be noted that the energy absorbtion by the pyrolysis gases as they pass through the char is important for most materials of interest. It is therefore important to choose an accurate model to obtain a gas enthalpy curve. In the present model tables of temperature versus gas enthalpy are required as input.

iv) **Porosity** : The evaluation of porosity of a material is basic and is calculated by using the change in density divided by the original density via

$$\phi = \phi^o + \frac{d\rho}{\rho} \qquad (4.6)$$

However the present model uses tabulated values of porosity versus the degree of char.

v) **Degree of char** : The degree of char is a parameter for describing a partially pyrolysed component. It is given by

$$\beta(t) = \frac{\rho_v - \rho}{\rho_v - \rho_c} \qquad (4.7)$$

The properties associated with the storage term were evaluated as a function of the relevant parameters of the control volume. The properties associated with the flow term at the control volume boundaries were evaluated as a function of the relevent interpolated parameters at the boundaries

4.4 Pore Pressure Schemes

The highly non-linear pressure equation is shown as in Eq (2.19)

$$\frac{\partial}{\partial t}\left(\frac{\phi M A_c}{Z R T} P\right) = \frac{\partial}{\partial x}\left[\left(\frac{K}{\mu\gamma}\right)_e (\rho_g)_e A \frac{\partial P}{\partial x}\right] - A_c \frac{\partial \rho}{\partial t}$$

As stated earlier, one objective of this study is to propose a procedure which will result in a time accurate pore pressure prediction. The highly nonlinear nature of the pressure equation along with the fact that the permeability of the material changes by several order of magnitudes are the key reasons for focusing on procedures for evaluation of properties used in that equation. The diffusion term in Eq. (2.19) represents the net rate of flow of gas into the control volume. The gas mass flow rate at any control volume face is the product of velocity, gas density and the flow area. The compact form of the Darcy-Forcheimer model for flow through porous media Eq. (2.17) is similar to Fourier's law for conduction heat transfer. Therefore, as far as gas velocity calculation is concerned, we need a model for evaluation of effective conductance for flow between two adjacent control volumes. Figure 4.4 illustrates two adjacent unequal control volumes. There are numerous ways by which one can calculate an effective conductance for flow with velocity of u_i between nodes P_i and P_{i+1}. Three ways for calculation of the effective conductance for flow will be discussed.

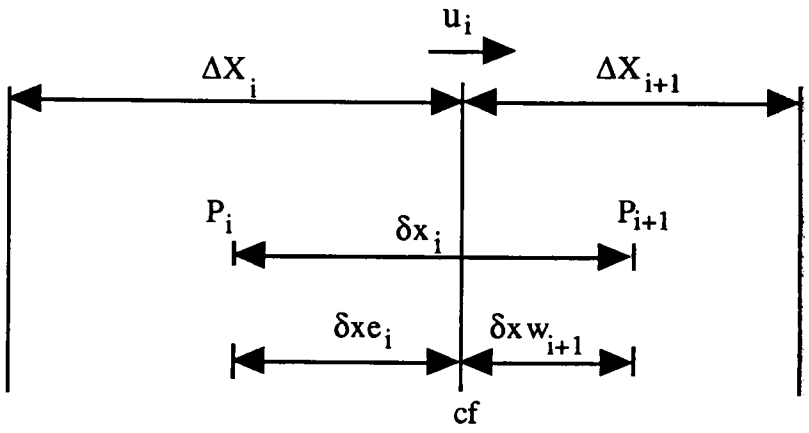

Fig 4.4 Pore pressure control volumes

4.4.1 Harmonic Mean of Flow Conductances

Patankar (1980) proposes use of harmonic mean of conductances when there is a large difference between the thermal conductivity of two adjacent control volumes. Following the resistance concept for calculation of the effective conductance for flow, the following expression for the effective flow conductivity is obtained,

$$\left(\frac{K}{\mu\gamma}\right)_e = \frac{\left(\frac{K}{\mu\gamma}\right)_{i+1}\left(\frac{K}{\mu\gamma}\right)_i}{\left(\frac{K}{\mu\gamma}\right)_{\ell,cf}} \qquad (4.8)$$

where

$$\left(\frac{K}{\mu\gamma}\right)_{\ell,cf} = \frac{\delta xe_i\left(\frac{K}{\mu\gamma}\right)_{i+1} + \delta xw_{i+1}\left(\frac{K}{\mu\gamma}\right)_i}{\delta xe_i + \delta xw_{i+1}} \qquad (4.9)$$

In these equations the degree of char of a control volume is used to obtain its permeability from the input data file. Similarly, the temperature of the control volume is used to obtain the gas viscosity for that control volume.

4.4.2 Modified Harmonic Mean of Flow Conductances

The permeability data is measured at various degrees of char. The degree of char changes from zero to unity while the corresponding change in the permeability may be as much as seven order of magnitudes. Therefore, it is possible to have adjacent control volumes with substantial difference in their respective permeabilities. The weakness of harmonic mean method lies with the value of the denominator which is supposed to represent the true value at the control volume face. In the modified harmonic mean method, we simply propose to evaluate the denominator in Eq. (4.8) at the degree of the char of that location. Calculations show that there is vast difference between the interpolated value Eq. (4.9) and the value obtained using the degree of the char of the control volume face. The modified form of Eq. (4.8) is

$$\left(\frac{K}{\mu\gamma}\right)_e = \frac{\left(\frac{K}{\mu\gamma}\right)_{i+1}\left(\frac{K}{\mu\gamma}\right)_i}{\left(\frac{K}{\mu\gamma}\right)_{cf}} \qquad (4.10)$$

where cf stands for value evaluated at the control volume face using the degree of char and temperature values at that location.

4.4.3 Weighted Average of Flow Conductivities

This method is based on the simple concept that each control volume contributes to the effective $K/\mu\gamma$ according to its volume in the path of the gas. The equation for this method is

$$\left(\frac{K}{\mu\gamma}\right)_e = \frac{\delta xe_i\left(\frac{K}{\mu\gamma}\right)_i + \delta xw_{i+1}\left(\frac{K}{\mu\gamma}\right)_{i+1}}{\delta xe_i + \delta xw_{i+1}} \qquad (4.11)$$

Clearly there are other candidates for the effective flow conductivity such as the denominators of Eqs. (4.8) and (4.10), or even the value of $K/\mu\gamma$ at node i or i+1. The weakness of these selections as well as the weighted average method lies in the fact that none of them can account for a situation where one of the adjacent control volumes is nearly impermeable. It should be noted that the harmonic mean concept will result in a zero effective flow conductivity when one of the adjacent control volumes is impermeable.

Three schemes for calculation of the gas velocity at the control volume boundary have been established. Now one can focus on the gas density at which the fluid crosses the control volume boundary. There are two logical choices for the calculation of the gas density crossing the control volume boundary.

1.) Using the interpolated values for temperature and pressure at control volumes interface to calculate $(\rho_g)_e$. This procedure should be used when one is solving a pressure equation, i. e., piecewise-linear in pressure and temperature. If one is solving an equation in terms of gas density, i. e., piecewise-linear in gas density and temperature, then the appropriate value for $(\rho_g)_e$ is the interpolated value using the ρ_g of the adjacent control volumes.

$$(\rho_g)_e = \left(\frac{PM}{ZRT}\right)_{cf} \qquad (4.12)$$

2.) The second scheme for calculation of $(\rho_g)_e$ is based on the upwind concept, i. e., the density of the gas crossing the control volume boundary is equal to its upstream value.

The combinations of the three proposed schemes for calculation of effective flow conductivity and the two schemes for calculation of the effective gas density results in six possible ways of solving the pore pressure equation. The details of the proposed methods are given in Table 4.1.

Table 4.1 Details of proposed methods

Method	Effective conductance	Effective gas density
a	Harmonic mean	Based on face temp, and pressure
b	Harmonic mean	Upstream value of gas density
c	Modified Harmonic mean	Based on face temp, and pressure
d	Modified Harmonic mean	Upstream value of gas density
e	Weighted average	Based on face temp, and pressure
f	Weighted average	Upstream value of gas density

4.5 Algorithm for Surface Temperature Determination

Before the description of the algorithm and flow chart for the solution scheme, a brief note must be made on the development of the linear expression $q_{bound} = AT_w + B$ where A and B are obtained from the indepth solution. As described earlier the finite difference expressions are obtained by integrating the final conservation equations in time and space. For each control volume the finite difference equation would have three

coefficients, the coefficient at the point and communication with the neighbours on either side. Therefore the entire domain would form a tridiagonal matrix. The final matrix would look like the one shown below, n equations corresponding to n control volumes which have to be solved simultaneously for the n unknowns.

$$\begin{bmatrix} D_1 T_1 + A_1 T_2 \\ B_2 T_1 + D_2 T_2 + A_2 T_3 \\ B_3 T_2 + D_3 T_3 + A_3 T_4 \\ \ddots \\ B_6 T_5 + D_6 T_7 + A_6 T_6 \\ \ddots \\ B_N T_{N-1} + D_N T_N \end{bmatrix} = \begin{bmatrix} C_1 + q_{bound} \\ C_2 \\ C_3 \\ C_6 \\ C_N \end{bmatrix}$$

It may be observed that beginning with the last node, the highest indexed unknown temperature may be eliminated from each equation in turn. This may be noted as the standard first step in the routine reduction of a tridiagonal matrix. The matrix is backsolved to reduce the indepth matrix to a linear expression of the form,

$$q_{bound} = AT_w + B \qquad (4.13)$$

where T_w is to be obtained from the boundary condition.

The algorithm for determination of the surface temperature is described below.

Surface energy balance equation is :

$$AT_w + B = q_{bound} \qquad (a)$$

Equation (a) is solved for T_w :

$$T_w = (q_{bound} - B) / A \qquad (b)$$

The function $F(T_w)$ representing the error associated with T_w calculation is given by :

$$F(T_w) = T_w + B/A - q_{bound}/A \qquad (c)$$

F' is computed by :

$$F'(T_w) = dF/dT_w = 1 - (1/A)(dq_{bound}/dT_w) \qquad (d)$$

Iteration Scheme:

(1) Using the latest values of B'_g and T_w an iterative q_{bound} value is determined from the surface heat flux table.

(2) An iterative T_w is computed by Eq. (b).

(3) $F(T_w)$ is computed via Eq. (c).

(4) Using the surface heat flux table the forward difference derivative of q_{bound} with respect to T_w is calculated at the iterative T_w value, and $F'(T_w)$ is obtained from Eq. (d).

(5) Using Newton Raphson iterative technique, T_w is updated via :

$$T_w = T_w - F(T_w)/F'(T_w) \qquad (e)$$

If $F(T_w)$ does not satisfy the convergence criterion, steps 1 to 5 are repeated. The converged T_w value is located at the intersection of the surface heat flux profile for a given B'g and the in-depth result, i.e., $q_{cond} = AT_w + B$ line. This is demonstrated in Fig 4.5.

4.6 Surface Ablation

It is assumed that ablation is a process of removal of material from the surface. Ablation may occur due to combined decomposition and char formation on the surface. The film coefficient model is based on the assumption that the surface recession is proportional to the amount of char injected to the surface. Since analytical investigation into the process

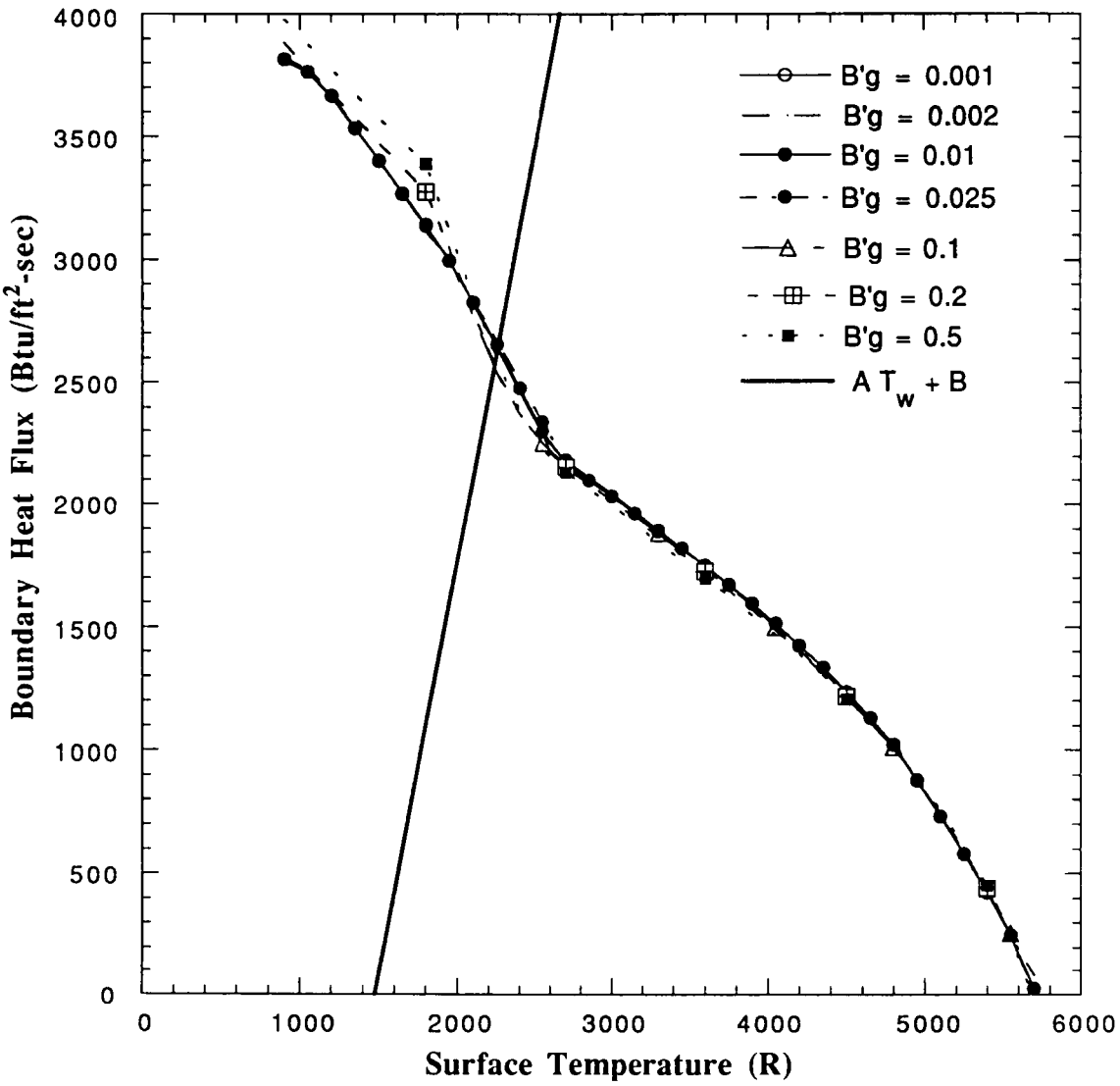

Fig 4.5 Determination of the surface temperature

is not practical because of the non-linear and complex nature of the governing equations, a numerical technique is proposed. Since analytical investigation into the process is not practical because of the non-linear and complex nature of the governing equations, a numerical technique is proposed.

The numerical technique proposed is convenient and does not incorporate the surface recession term in the governing equations. This way we can avoid the cumbersome coordinate transformation. The solution domain is divided into a number of non overlapping control volumes where the surface is a half control volume with a node assigned to the surface. As the process of ablation begins the control volume on the surface is reduced. The current size of the control volume and nodal distance from the neighbouring nodes are calculated. This in turn changes the effective conductance and storage of the control volume. It should be noted that as the surface control volume is completely removed, the adjacent control volume size is updated, this process continues till the surface node has reached its neighbours, then and the surface node index is increased by one.Thus effective number of equations are reduced by one and so on. A schematic of the process for the surface location is shown in Fig 4.6.

4.7 Solution Scheme

a) The material is initialized with the parameters necessary for the computation of the energy and pressure.

b) Time is stepped.

c) The nodal decompositions of the material are computed using the exact expression for the density change. Using the new density, then the new porosity and degree of char are computed.

d) Using the nodal $d\rho/dt$ obtained by the decomposition routine the pressure equation is solved. The modified harmonic mean concept with density of the gas evaluated at

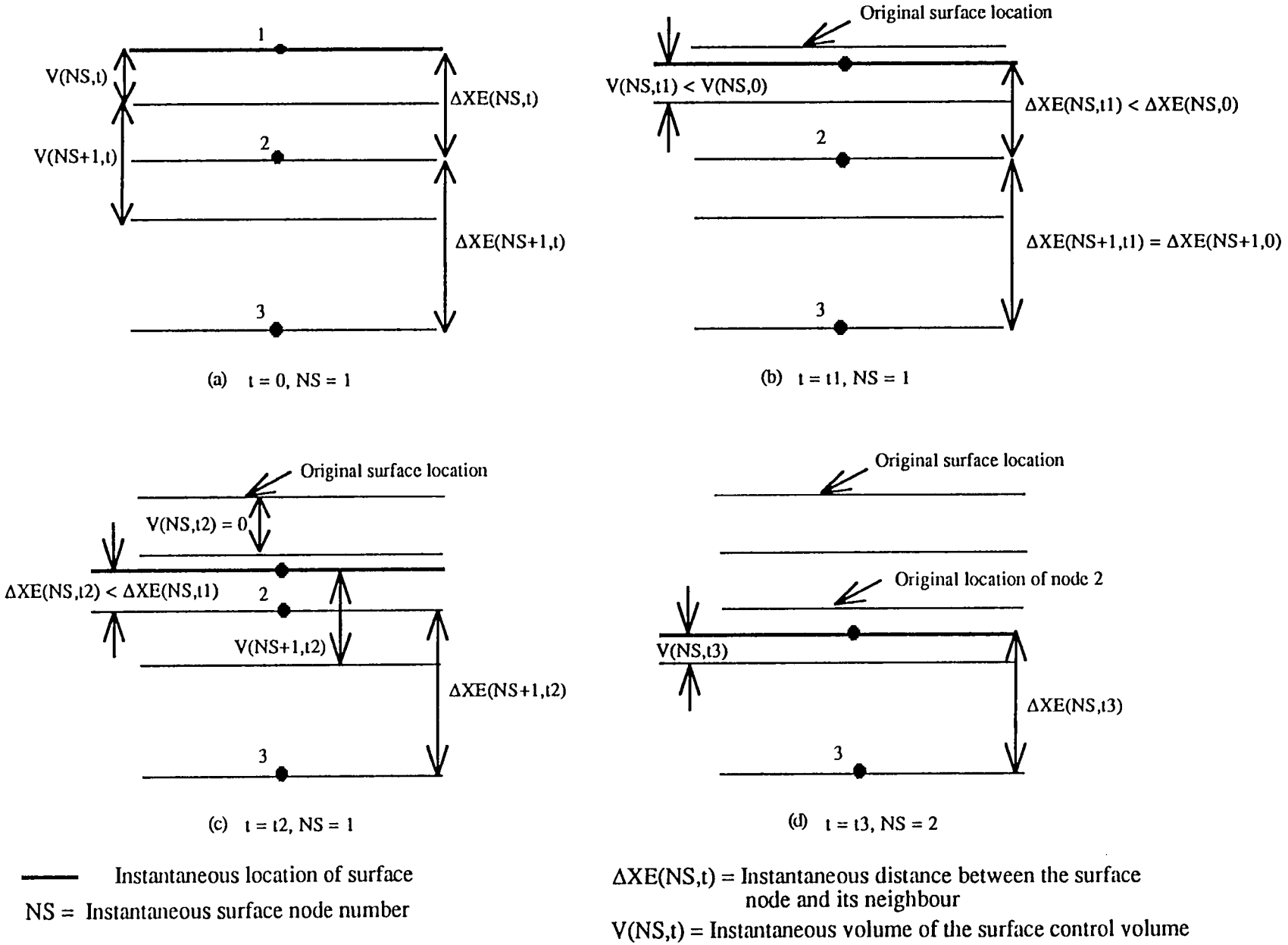

Fig 4.6 Sequence of computational steps for tracking the receding surface

the control volume face is used for the pressure solution to convergence. Using the converged pore pressure values the velocity of the gas at each control volume face is calculated. The mass flow rates are then calculated based on the velocities obtained and the densities of the gas taken at the appropriate locations.

e) Using the gas mass flow rates, the finite difference coefficients of each control volume for the energy equation are generated. The inverse tri-diagonal matrix algorithm is used to generate the equation $q_{cond} = A\ T_w + B$. Here A and B are obtained as a part of the in-depth solution. For the general boundary condition the temperature is obtained directly. But for the thermochemistry type boundary condition the surface temperature has to be iterated upon for the converged char mass flow rate and the surface temperature.

f) Based on the algorithm for the surface balance, the surface temperature is computed. The mass of char injection to the surface is also computed.

g) With the knowledge of surface recession the new domain of the problem is defined. The procedure for the handling of the surface recession was discussed in section (4.6). At this point one time step calculation are complete. A flow chart of steps involved in the computation are shown in Fig 4.7.

4.8 Test Cases

The following are the test cases used to evaluate the performance of the model and compare its predictions with CMA (Charring Material Ablation) code. CMA code was developed by Acurex Corporation and is widely used in the solid rocket nozzle community. The cases described are chosen so that complete working and performance of the model is shown.

a) **Sample1 :** This problem is meant to show the effect of the various pressure schemes, the effect of nodelets, effect of fully coupled and weakly coupled solution on the

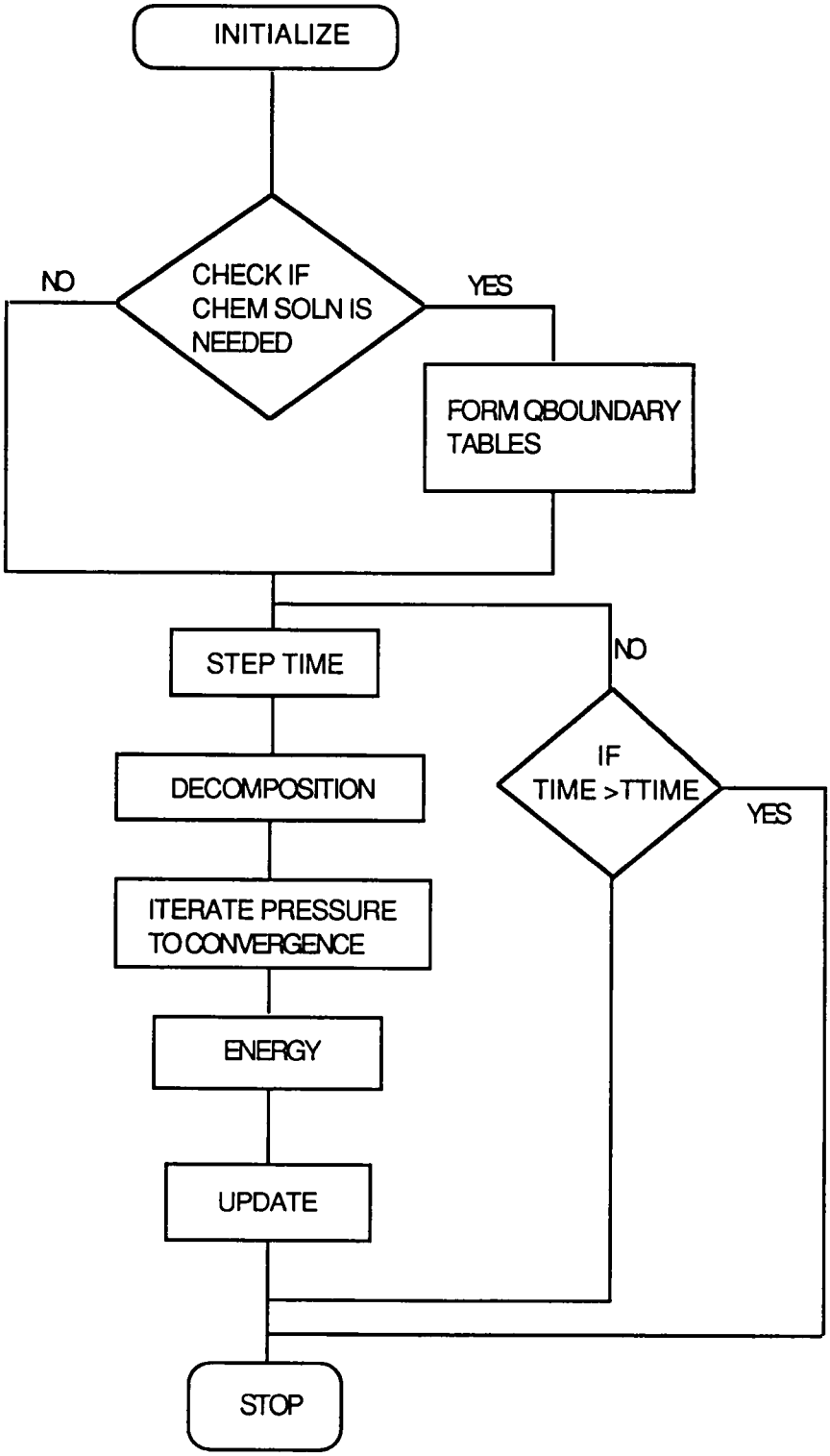

Fig 4.7 Flow chart for the computation

indepth profiles. The effect of advection is also shown.

b) **Sample2 :** This problem demonstrates the effect of the chemically reacting boundary layer. The ablation routine and the algorithm for surface temperature determination is tested.

c) **Sample3 :** This problem shows the capability of the model for handling multi-material domain. The surface is subjected to a chemically reacting boundary layer with ablation.

d) **Sample4 :** This problem demonstrates the capability of the model to handle a fixed surface recession rate with constant temperature and pressure boundary conditions on either faces.

e) **Sample5 :** This problem demonstrates the use of a general type of boundary condition, Eq. (3.1), in this case a constant heat flux boundary condition. The other face of the material is insulated but held at a constant pressure.

CHAPTER 5

RESULTS AND DISCUSSION

In order to show the effect of various schemes on the predicted pore pressure field the following computational experiment was performed.

5.1 Test Case One

The selected test problem, shown in Fig. 5.1, is a slab of composite with a thickness of L=1.0 cm at initial temperature and pressure of T_{in} =300 K and P_{in} =1 atm. The temperature at x=0 is suddenly raised to T_s =3000 K with P_s =P_{in} , while the surface at x=L is maintained insulated and impermeable.

5.1.1 Input Data

The data used in the test problem are given in Tables 5.1-5.3. Table 5.1 presents the constants for the nth order kinetic rate equations which were used for modeling the decomposition process. The temperature and degree of char dependent material properties are shown in Tables 5.2 and 5.3, respectively. The Ergun coefficient C_E was set to zero (Darcy Flow model, γ = 1), and the pyrolysis gas was assumed to obey ideal gas law (Z=1). It should be noted that the material properties use in this paper are not for any specific composite. Nonetheless, they are in a realistic range for low permeability carbon reinforced polymers. Units for this problem are in the metric system.

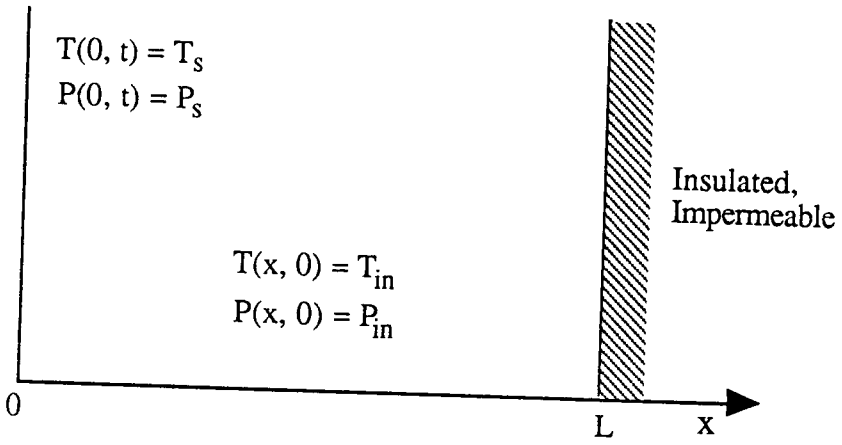

Fig. 5.1 Description of the test problem one

Table 5.1. Reactions Kinetic Constants, $\Gamma = 0.4$

Component (i)	Virgin density	Char density	Pre exponential factor	Order of reaction	Activation energy	Cut off temperature
1	245.0	0.0	20.0	2.0	4600.0	310.0
2	0.0	0.0	-	-	-	-
3	2230.0	1900.0	9.0E+10	3.0	19300.0	560.0

Table 5.2. Temperature Dependent Material Properties

Property	Virgin		Char		Pyrolysis gas	
	300 K	3000 K	300 K	3000 K	300 K	3000 K
Thermal conductivity	1.5	8.0	1.5	8.0	----	----
Specific heat	1600.0	2500.0	1600.0	2500.0	3500.0	10000.0
Gas Viscosity	----	----	----	----	1.7E-5	8.0E-5
Molecular weight	----	----	----	----	17.0	11.0
Enthalpy of formation	- 9.0E+5	----	0.0	----	- 3.7E+6	----

Table 5.3. Degree of Char Dependent Material Properties, $C_E = 0$ (Darcy Flow Model, $\gamma = 1$)

Degree of char (%)	Solid bulk density	Porosity (%)	Permeability (m^2)
0.0	1436	1	5E-20
25	Eq. (2.2)	9.5	3E-18
50	" "	18.0	3E-17
75	" "	26.5	2E-16
100	1140	35	1E-13

A uniform mesh size of Δx = 0.5 mm with half control volumes located at the boundary nodes was used to obtain the results. The computations were carried out with a time step of 0.025 s., and terminated at t = 2 s. Since the objective of this work is to study the effects of various schemes on pore pressure predictions, it was decided that short transient results were sufficient to meet the stated objective.

5.1.2 Pore Pressure Schemes

The predicted pore pressures at t = 0.2 s and t = 2.0 s are presented in Figs. 5.2(a,b), respectively. It can be seen that the variation in the predicted pressures by the six proposed methods is as much as five folds. For a given scheme for calculation of effective flow conductivity, the choice of upstream value for gas density crossing the control volume boundary results in a major reduction in the predicted pore pressure (compare methods a and b, c and d, e and f). It is further observed that the weighted average scheme and the harmonic mean scheme are using the highest and the lowest effective flow conductivities, respectively, for velocity calculation. It should be noted that any scheme that can not result in $(K/\mu\gamma)_e = 0$ when one of the adjacent control volumes is impermeable is not acceptable. Therefore, the "correct" scheme must be based on harmonic mean concept. As stated earlier, the permeability is a highly nonlinear function of degree of char (Table 5.3). Thus, among the harmonic mean based schemes, the one which uses more β values for calculation of $(K/\mu\gamma)_e$ is preferred.

The corresponding predicted temperatures are nearly the same, and they are not distinguishable in a graph. The fact that the resulting temperature predictions are nearly the

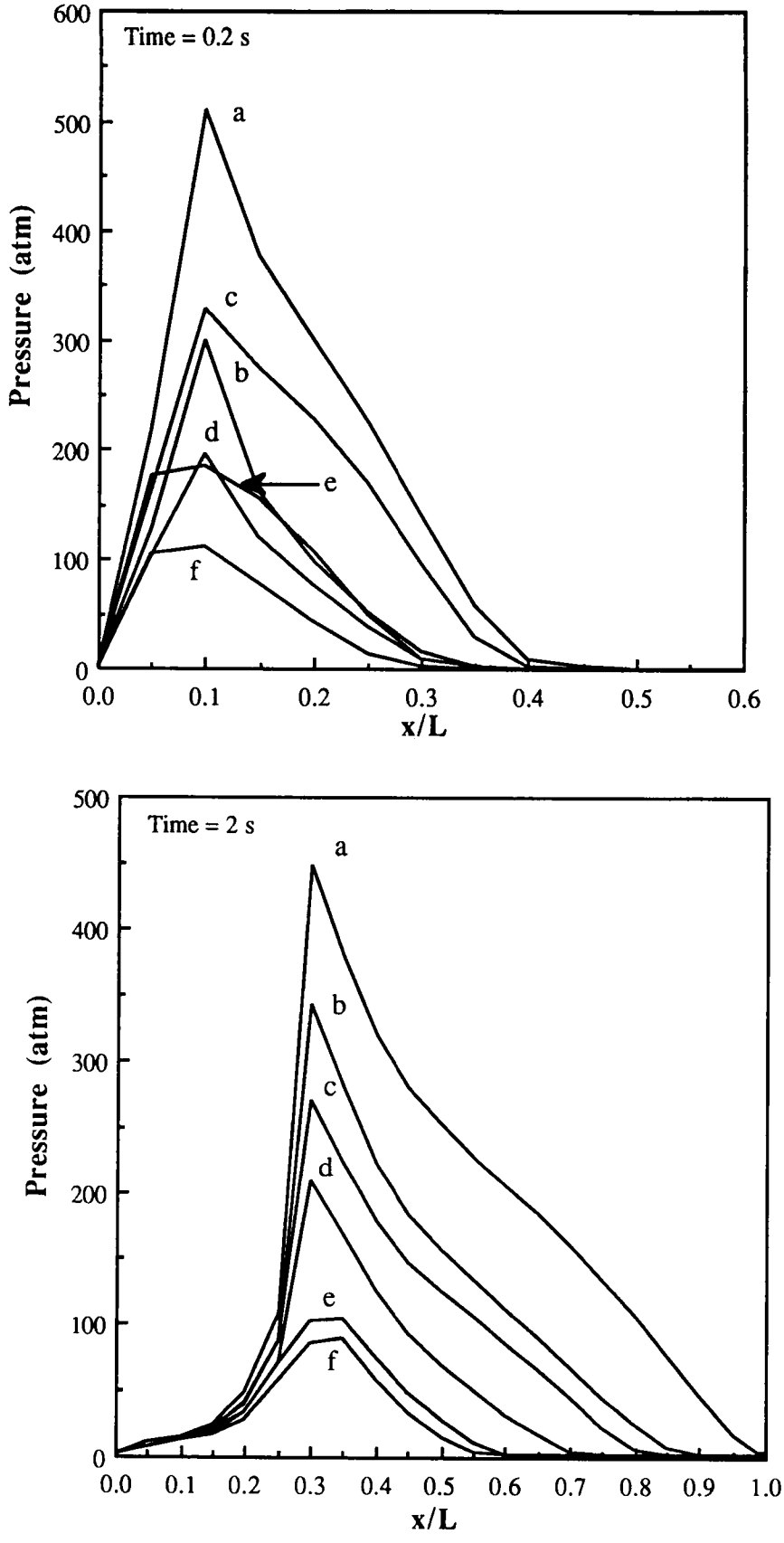

Fig.5.2 Predicted pore pressures by schemes a through f: (a) time = 0.2 s ; (b) time = 2.0 s

same while the pressures are substantially different can be explained as follows.

i) Advected energy is not the dominant factor in the heat transfer process. This point will be further discussed while presenting the limiting advection effect.

ii) Figure 5.2(a,b) shows that close to the surface the predicted pressures are close to one another, and thus the gas mass flow rates will be close, Fig 5.3.

iii) The scheme which is predicting a high pressure is using a low effective flow conductivity value which results in a low velocity. However, a high pressure yields a high gas density. Consequently, the gas mass flow rate, which is the product of a lower velocity and a higher gas density, does not vary much from that which is obtained from a low pressure field.

The above observation is supported in Fig. 5.3 which present the gas mass flow rates per unit area at t = 2 s. As can be seen, the predicted values for various schemes are very close to one another. It should be added that at t = 0.2 s the gas mass flow rates predicted by various schemes are nearly the same.

Florio and Henderson (1991) compared their predicted pore pressure field with the measured values by Ramamurthy (1988). Their predictions were generally much higher than the measured values. Florio (1989) used the following scheme in his pore pressure calculation.

$$\left(\frac{K}{\mu\gamma}\right)_e = \left(\frac{K}{\mu\gamma}\right)_{i+1} \quad , \quad \left(\rho_g\right)_e = \left(\rho_g\right)_{i+1} \qquad (5.1)$$

Figure 5.4 shows the comparison between the scheme (d) and Florio's scheme.

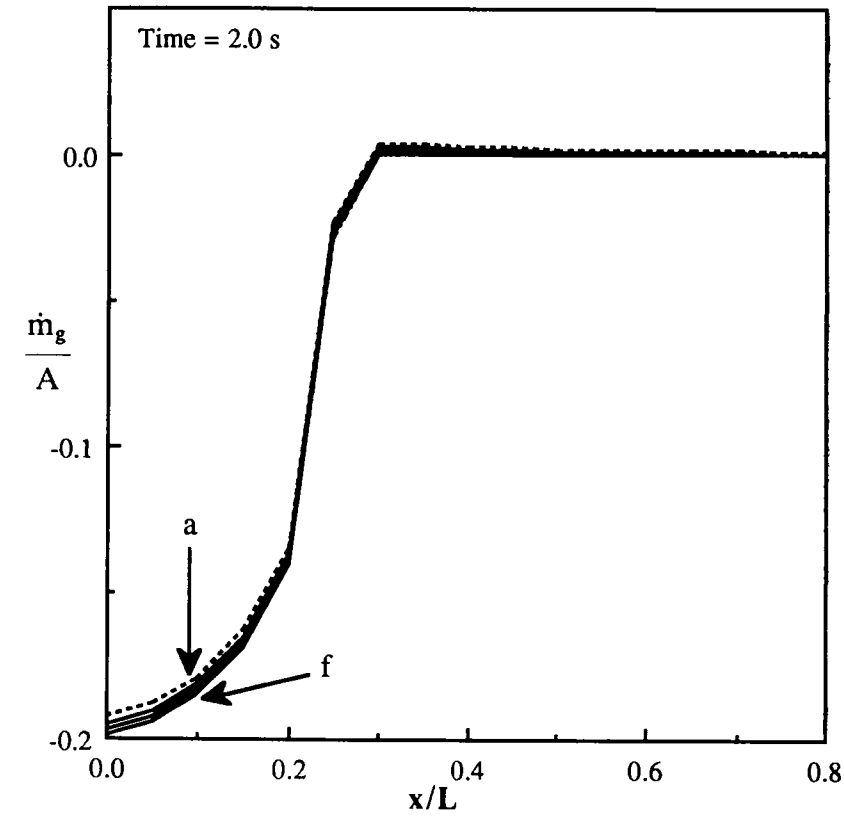

Fig. 5.3 Predicted gas mass flow rates per unit area by schemes a through f

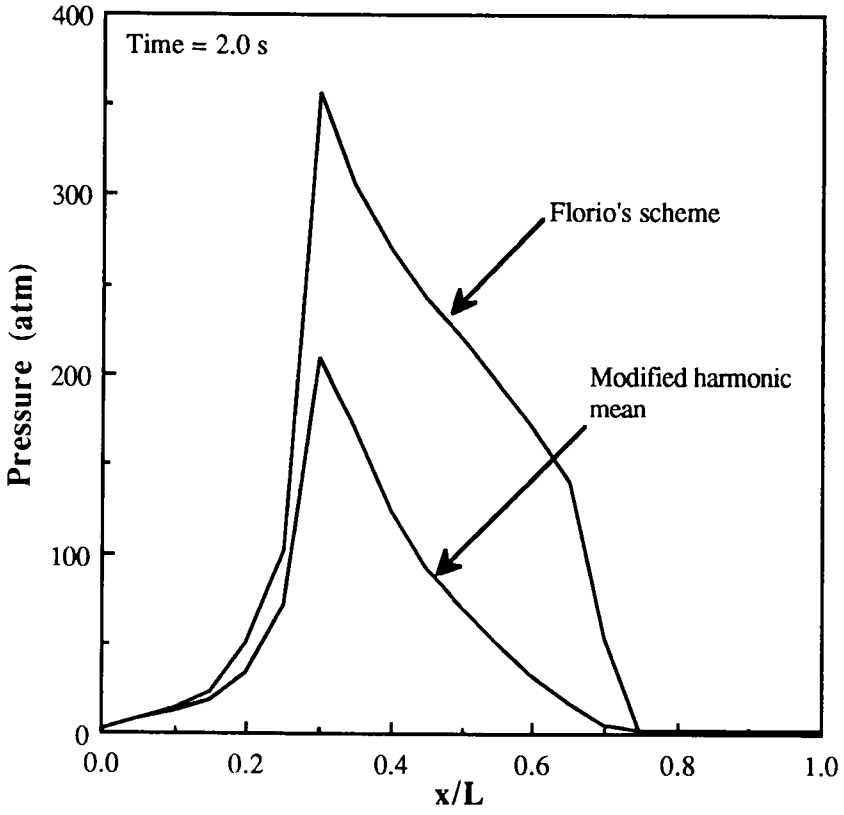

Fig. 5.4 Comparison of Florio's scheme with the recommended scheme

The figure shows that Florio's scheme predicts a maximum pressure at t = 2.0 s which is about 150 atm greater than the value predicted by the scheme (d). The remaining results to be discussed will be those of scheme (d).

The development of temperature and pore pressure profiles with time are presented in Figs. 5.5 and 5.6. As expected, with increasing time the location of maximum pressure moves further away from the heating surface, corresponding with the instantaneous location of the interface between the decomposition and virgin zones.

5.1.3 Nodelets Effect

The nodelets concept, i. e., calculation of gas mass generation based on a finer mesh using interpolated temperatures, was discussed earlier. All the gas mass calculations in the present study are based on 11 nodelets - of equal volumes- with a distribution of 5 nodelets on either side of the node. In order to show the nodelets effect on pore pressure prediction, a run was made without nodelets. The predicted pore pressures with and without nodelets at t = 0.2 and 2 s are presented in Figs. 5.7(a,b). At early times, the nodelets scheme predicts a substantially higher pore pressure field for the entire penetrated zone (Fig. 5.7a). As the material is penetrated with temperatures appreciably higher than the cut off values (which triggers the gas generation), the predicted pressures by the two schemes are very close to one another in the char region and most of the pyrolysis zone (Fig. 5.7b). At all times, the nodelets scheme predicted higher pressures in the region close to the end of pyrolysis zone and the adjacent virgin material. The nodelets scheme has negligible effect on the predicted temperature profile. This is due to items i and ii presented earlier in the pore pressure schemes section.

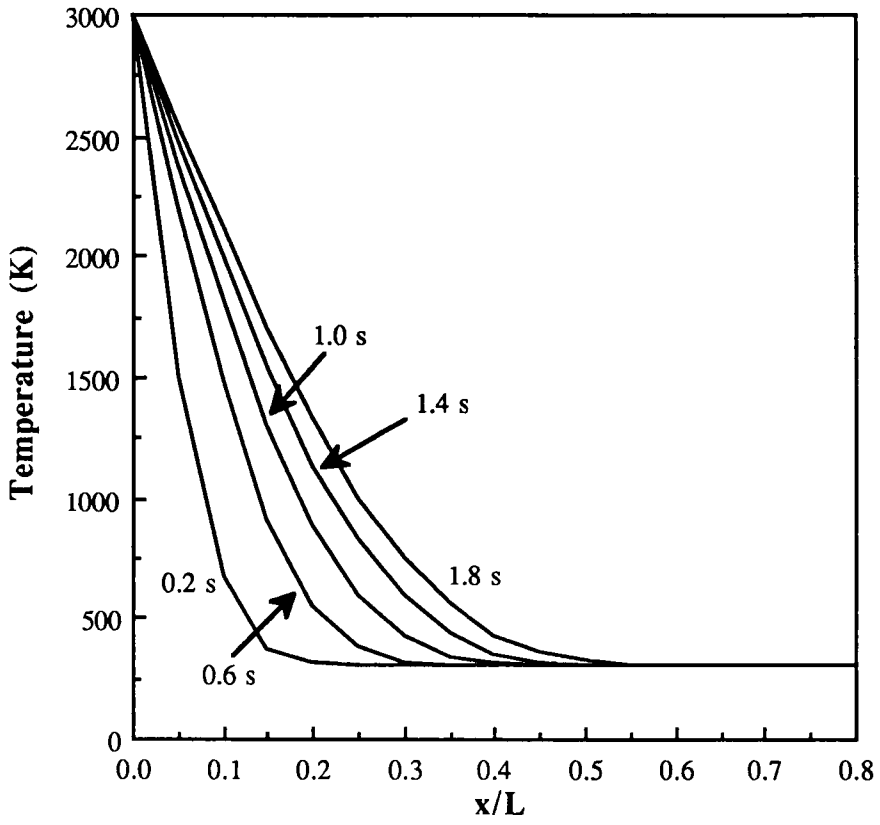

Fig. 5.5 Development of temperature profiles with time

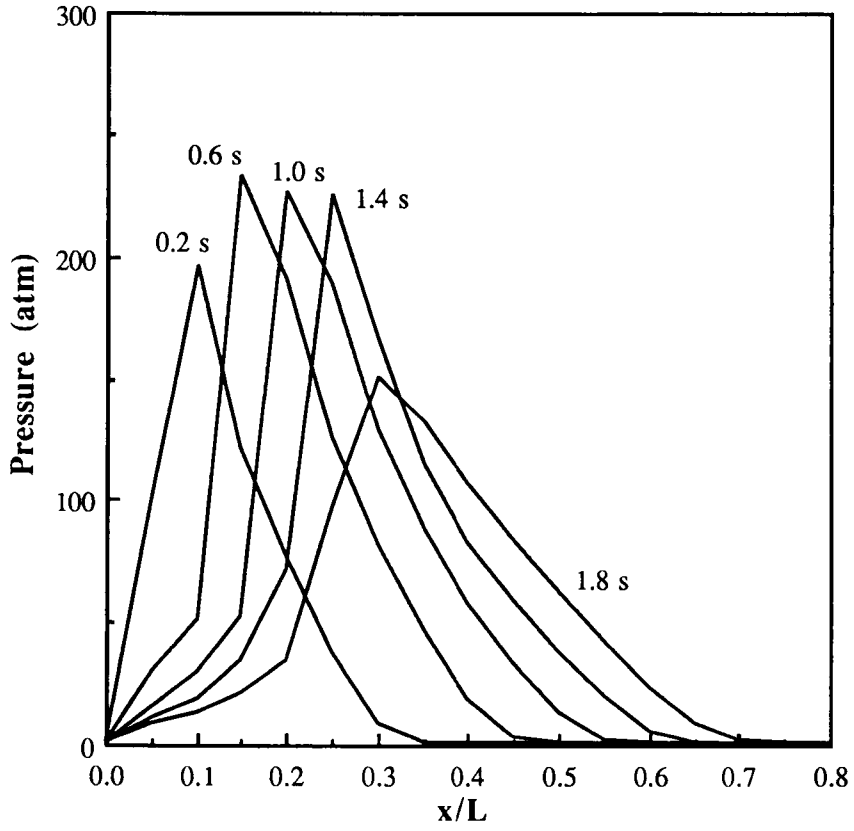

Fig. 5.6 Development of pressure profiles with time

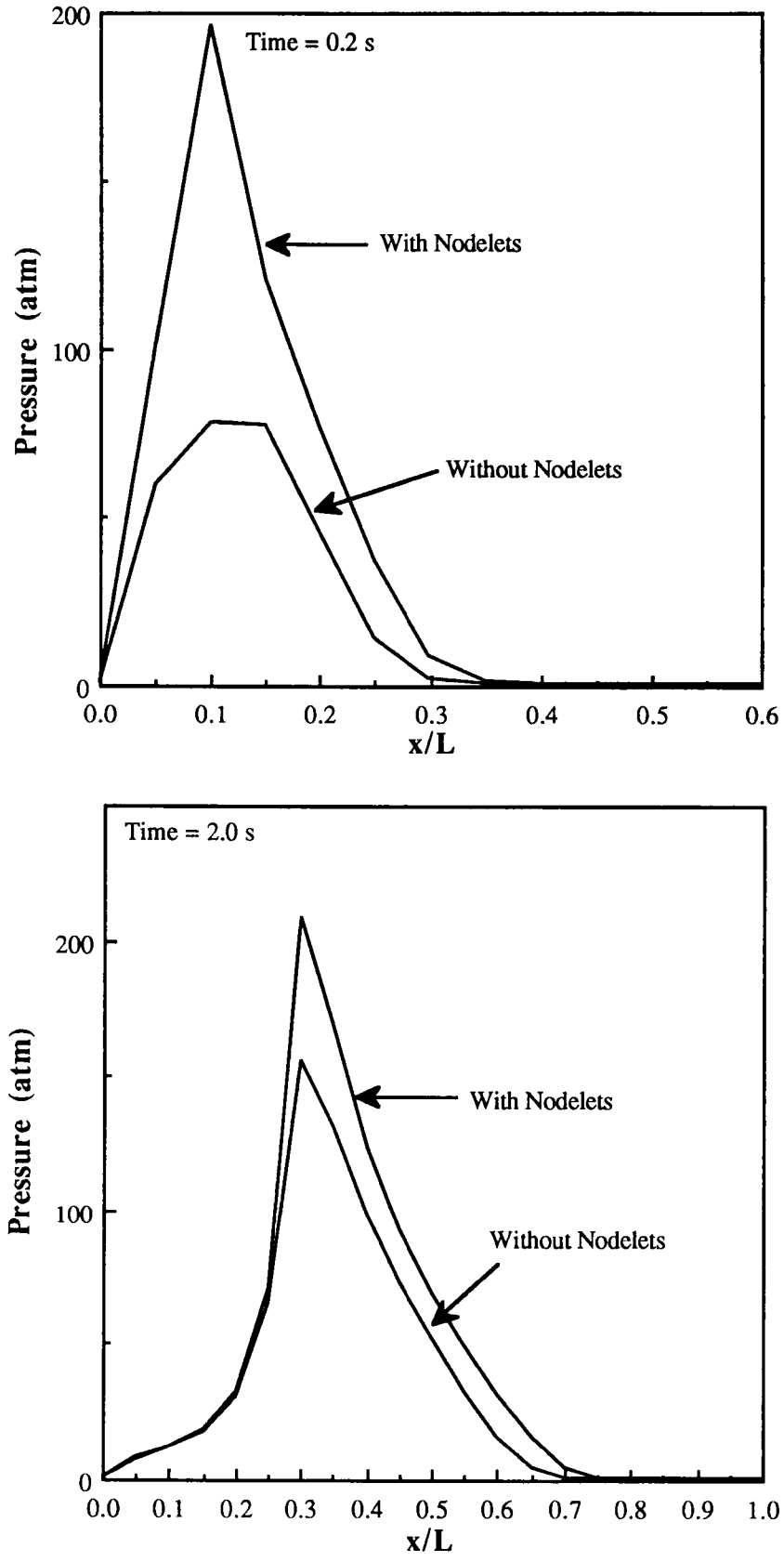

Fig. 5.7 The effect of nodelets scheme on the pressure solution: (a) time = 0.2 s ; (b) time = 2.0 s

5.1.4 Coupling Effect

In the general solution scheme section we described the calculation procedures for obtaining weakly coupled and fully coupled results. The weakly coupled and fully coupled pore pressure predictions at t = 0.2 and 2.0 s are presented in Figs. 5.8(a,b). At t = 0.2 s there is appreciable difference in the profiles for the entire penetrated region. With increasing time, the difference between the two profiles diminishes in the char zone and most of the decomposition region (Fig. 5.8b). At all times, the fully coupled scheme predicted higher pressures in the region close to the end of pyrolysis zone and the adjacent virgin material. The fully coupled scheme had a negligible effect on the temperature profile. It must be noted that clearly the difference between the two schemes depends on the magnitude of the time step.

5.1.5 Advection Effect

The heating of the composite is due to conduction phenomenon, while the endothermic decomposition and the advected energy by the pyrolysis gases - primarily towards the heated surface - serve as cooling processes. In order to quantify the cooling effects due to phase change δT and advection ΔT, the following computations were performed. A conduction solution was obtained via changing the cut off temperatures to values above 3000 K. We should mention that in order to ensure that the same thermal conductivity and specific heat values were used in the conduction solution, our input values for char and virgin material were chosen to be the same (Table 5.2). Next, we made a run which modeled the conduction and phase change processes. This was accomplished by changing the cut off temperature values back to the input values (Table 5.1), and passing zero gas mass flow rates from the pore pressure routine to the energy equation routine. The predictions for conduction, conduction and phase change, and full energy equation models are presented in Fig. 5.9 for t = 2.0 s. As expected the highest and the lowest predicted

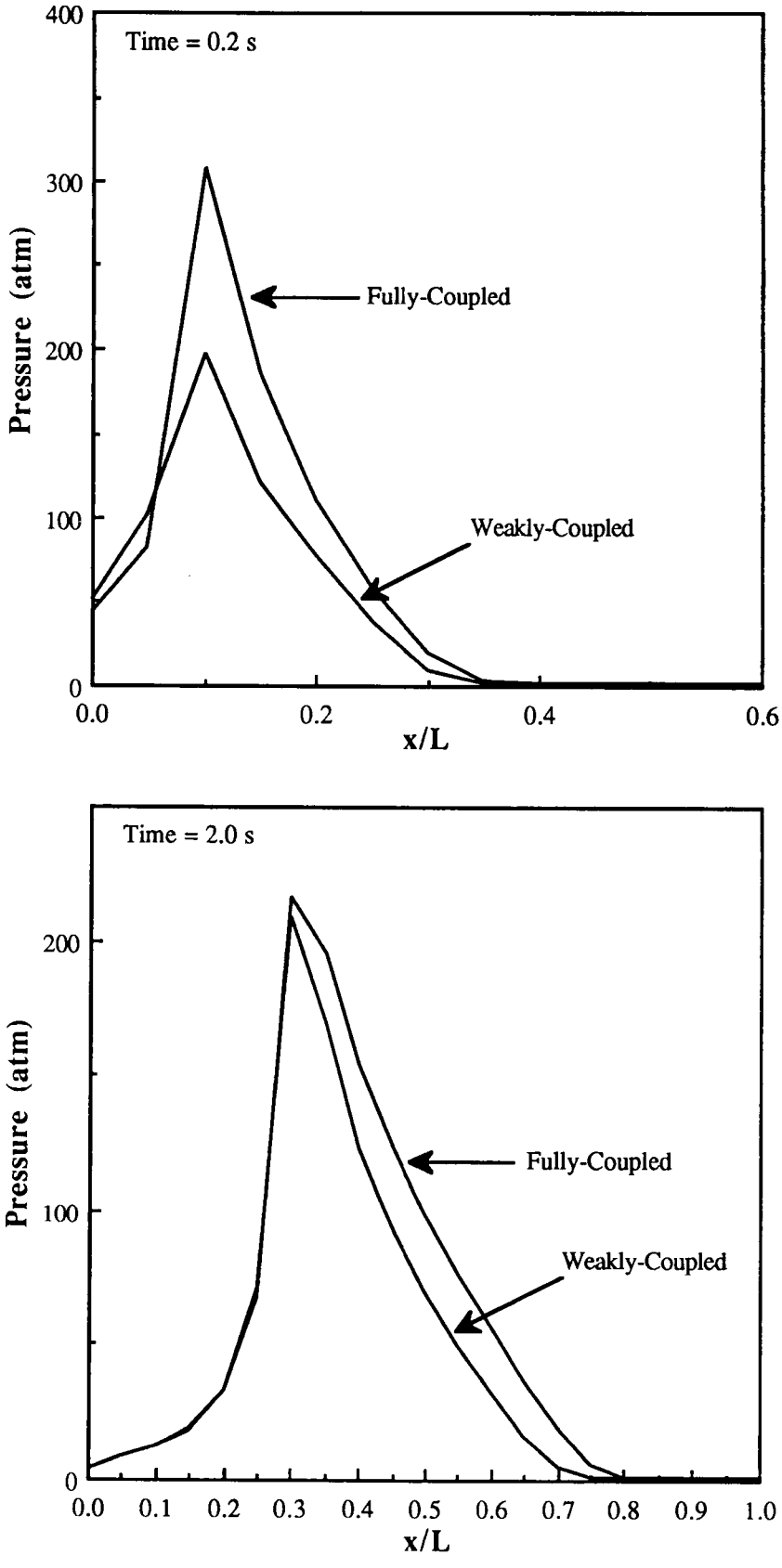

Fig. 5.8 Comparison of fully coupled and weakly coupled solution schemes on pore pressure: (a) time = 0.2 s ; (b) time = 2.0 s

temperature profiles are, respectively, due to the conduction solution and the full energy equation model. The conduction and phase change results are δT lower than the conduction solution, while a further drop in temperature (ΔT) from the conduction and change solution is due to the advected energy. The prediction of a two energy equations model for the solid temperature is delimited by the conduction and phase change solution and that of the full energy equation model (Eq. (2.14)). The phase change cooling δT and advection cooling ΔT spatial distributions at various times are presented in Figs. 5.10(a,b). As expected these profiles move inwards with the pyrolysis zone. The error associated with a one energy equation model versus two energy equations model clearly depends on the magnitude of the volumetric heat transfer coefficient between the solid and the gas, which clearly will be material dependent. Assuming that the two energy equations results would lie at mid value between the middle and the lower curves in Fig. 5.10, the approximate error will be less than 12 percent.

5.2 Test Case Two

The selected test problem, shown in Fig. 5.11, is a slab of composite with a thickness of L=0.1 ft at initial temperature and pressure of T_{in} =520 R and P_{in} =1 atm. The surface at x=L is maintained insulated and impermeable. The surface at x = 0 is subjected to a chemically reacting boundary layer, i.e., a variable flux input which is obtained via the thermochemistry tables.

5.2.1 Input Data

The Ergun coefficient C_E for this problem was set to zero (Darcy Flow model, γ = 1), and the pyrolysis gas was assumed to obey ideal gas law (Z=1). This study was conducted to compare the results of the present study with that of CMA. The input data

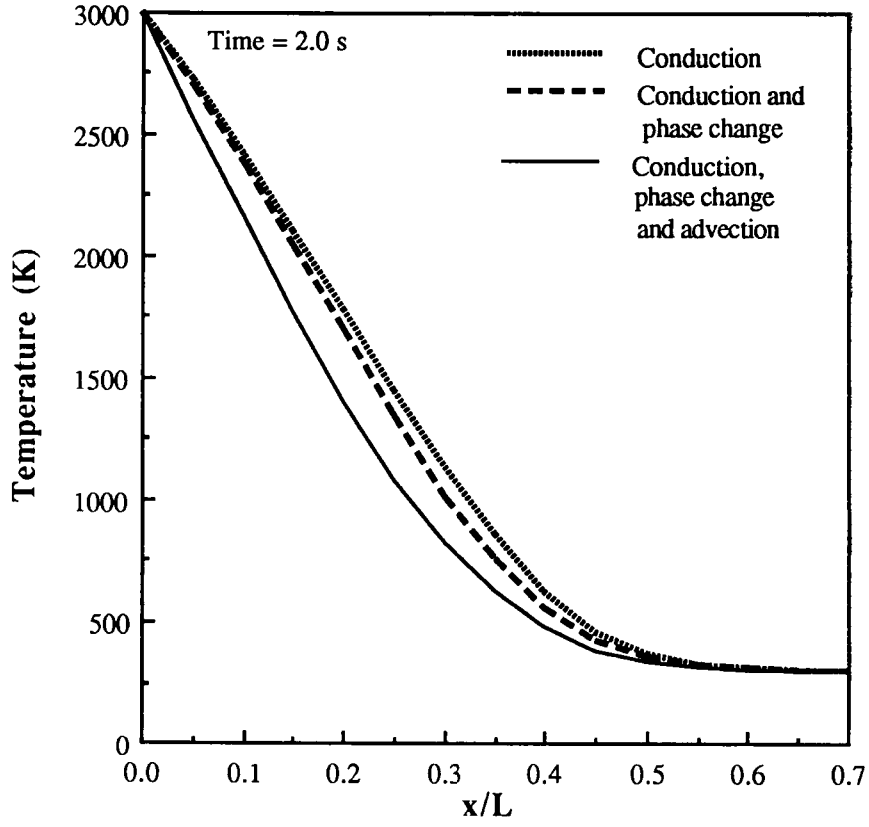

Fig. 5.9 Effects of phase change and energy advection on temperature profile

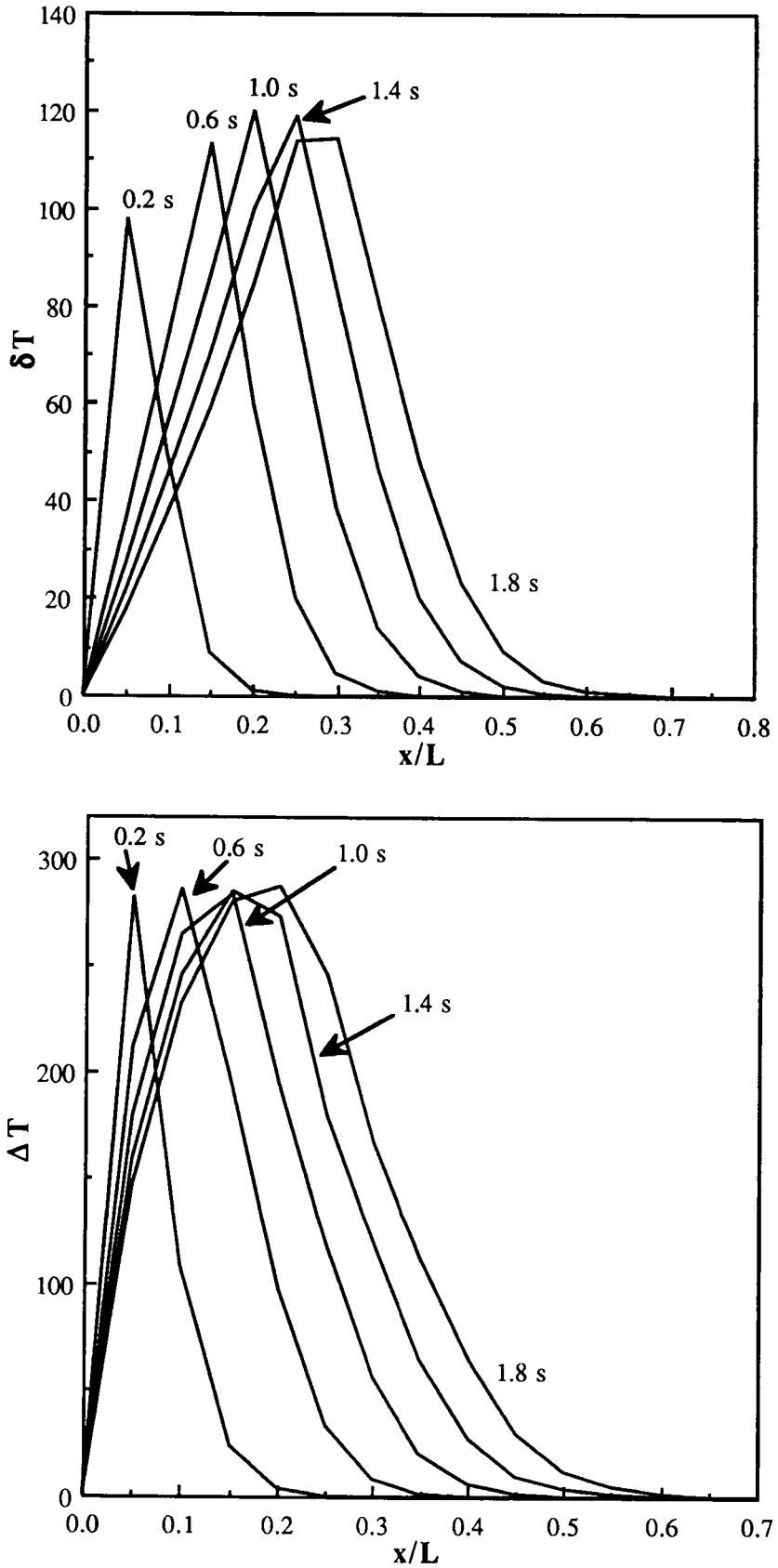

Fig. 5.10 The cooling effects of phase change (δT) and advection (ΔT): (a) phase change ; (b) advection

and thermochemistry table input for this problem are provided in the appendix A. The generated surface heat flux tables are also provided. The units for this problem are in foot poundmass and seconds.

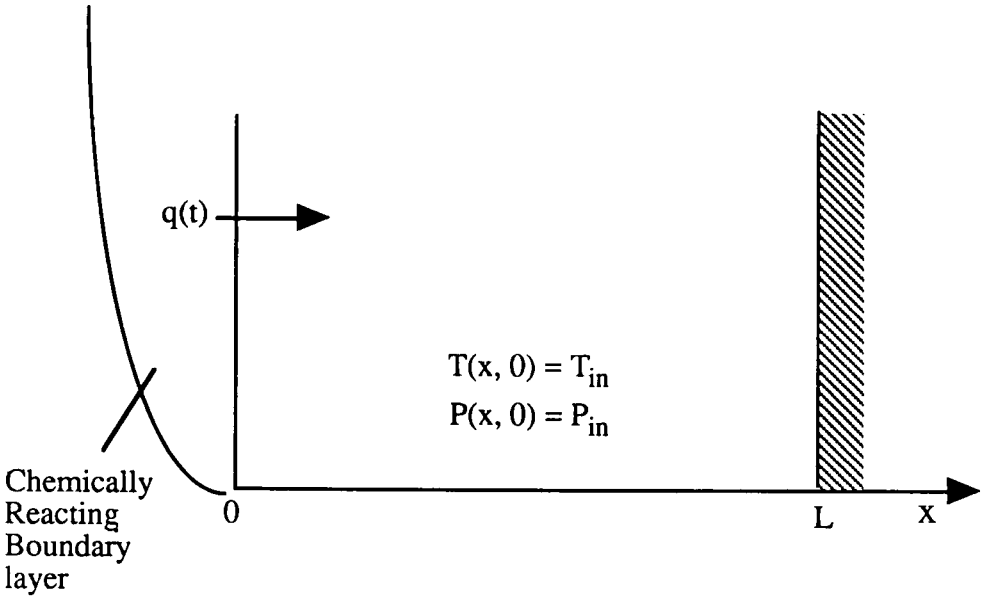

Fig. 5.11 Description of the test problem two

Comparisons of the predicted surface temperature, Recession rate and total recession with the CMA results are presented in Figs 5.12 to 5.14. The CMA results show an oscillation in the surface temperature, while the present study does not show any oscillation as seen in Fig(5.12). It can be observed that the surface temperature, recession rates and total recession compare well with CMA and are within 5%. The algorithm used for the determination of the surface temperature is stable and converges rapidly to a solution.

The oscillations in the surface temperature prediction of CMA could be attributed to the method of handling of the thermal conductivity. CMA uses the harmonic mean concept in determining the thermal conductivity at the face of the control volume. The

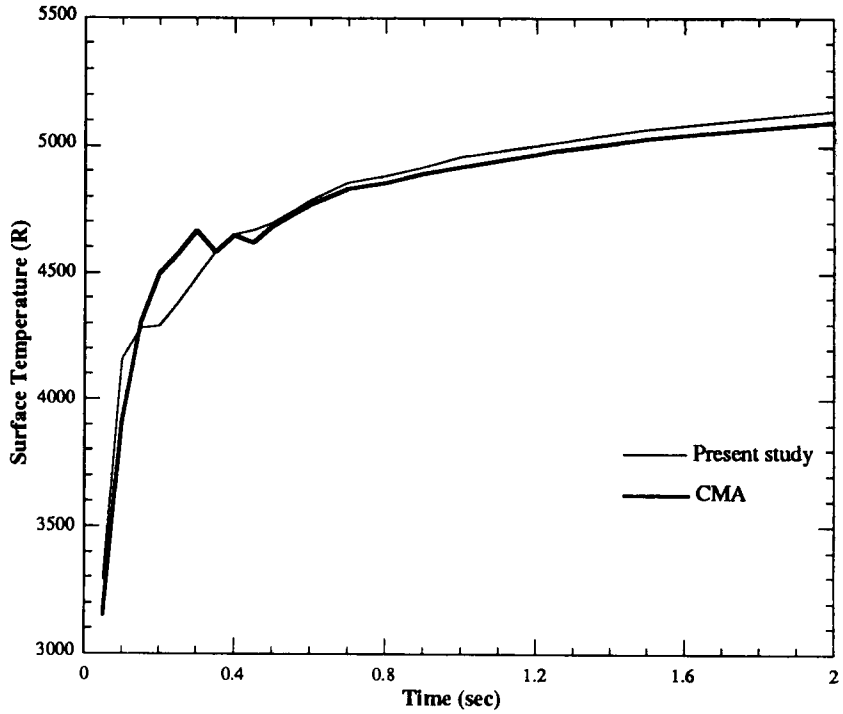

Fig 5.12 Comparison of the present study (surface temperature) with CMA

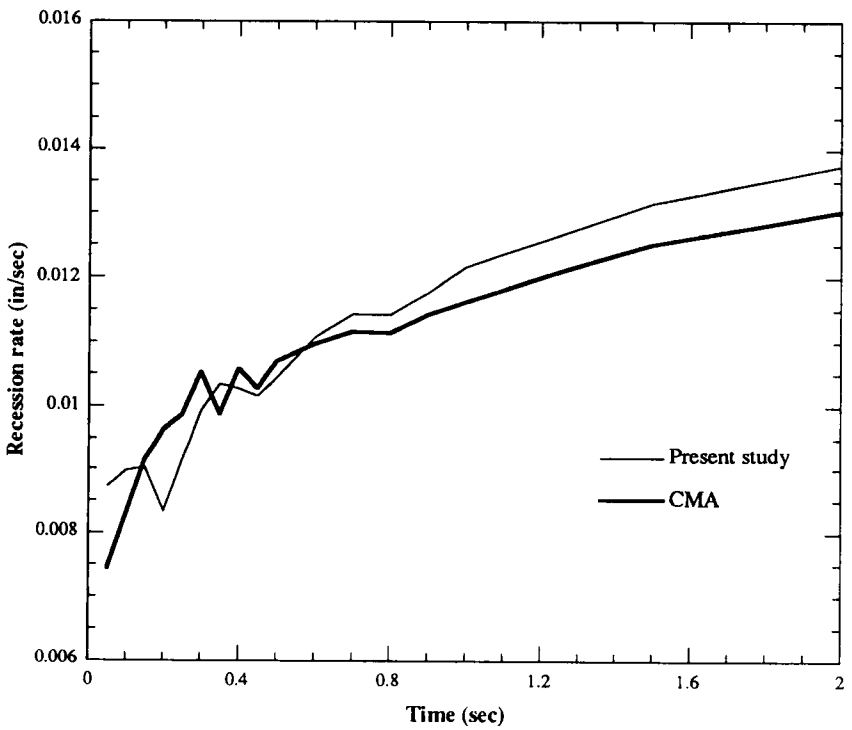

Fig 5.13 Comparison of present study (recession rate) with CMA.

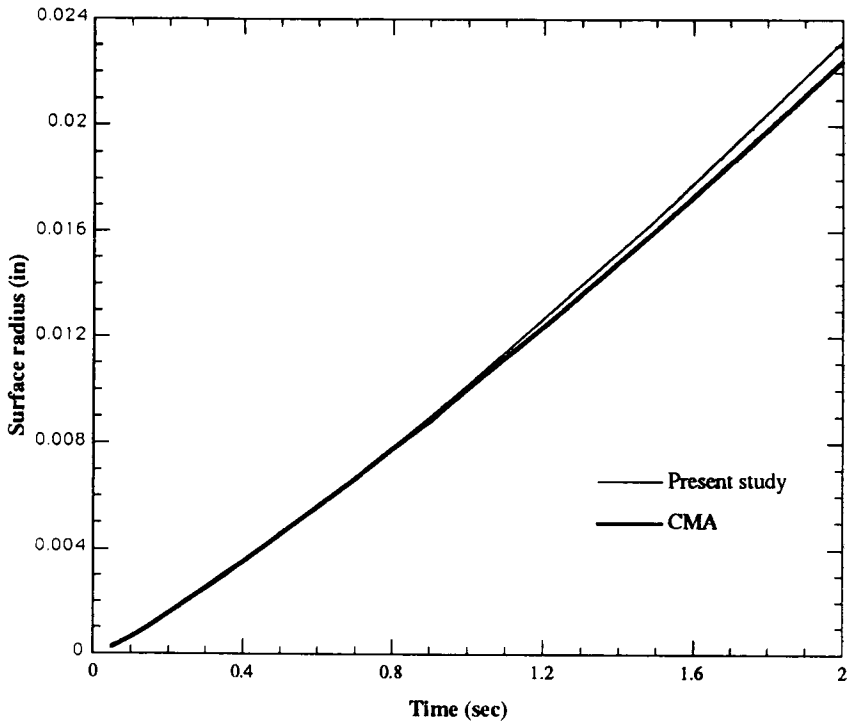

Fig 5.14 Comparison of present study (recession) with CMA

present study uses the average temperature concept in determining the thermal conductivity between two adjacent nodes. The present study uses the average temperature concept in determining the thermal conductivity between two adjacent nodes.

The recession rate as described earlier depends on the amount of char injected to the surface and could oscillate. From the relation for recession rate and total recesssion the total recession is a linear function of the time. The present prediction of the recession is very close to that of CMA.

The in-depth temperature and pore pressure predictions are shown in Figs 5.15 and 5.16, respectively. The temperature profiles compare well and are within 5 % . The large diferences in the pressure profiles is because CMA uses linear interpolation of flow conductances while the present study uses the modified harmonic mean of the flow conductances.

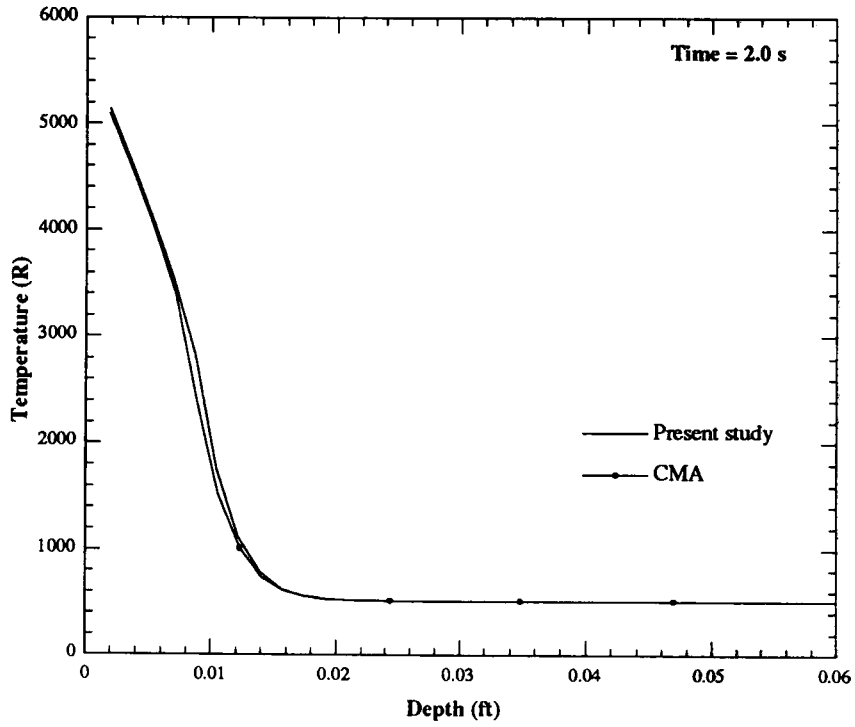

Fig 5.15 Comparison of in-depth temperature with CMA.

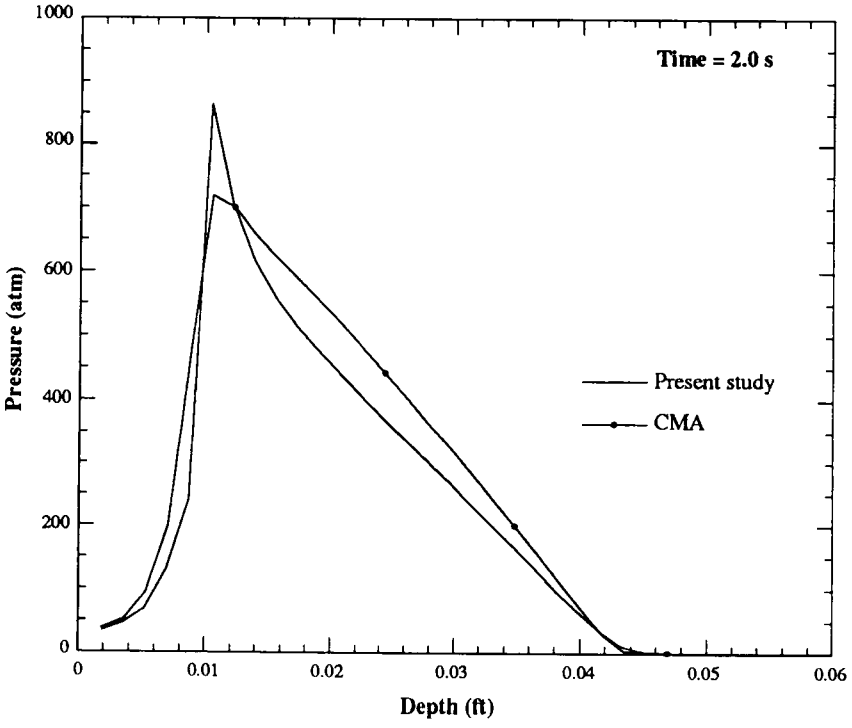

Fig 5.16 Comparison of in-depth pressure with CMA.

5.3 Test Case Three

The following test (fig. 5.17) is performed to show the capability of the model in handling multiple materials stacked one on top of the other. The figures provided show the temperature and pressure build up in a multiple material type configuration. The input data for this problem is provided in the appendix A.

There is recession at the surface which is subjected to a chemically reacting type boundary condition. Figures 5.18-5.19 show the development of the temperature and pressure profiles in the domain for time = 2, 6 and 10 s. The time step for this problem is 0.05 s. The units are in foot poundmass and second.

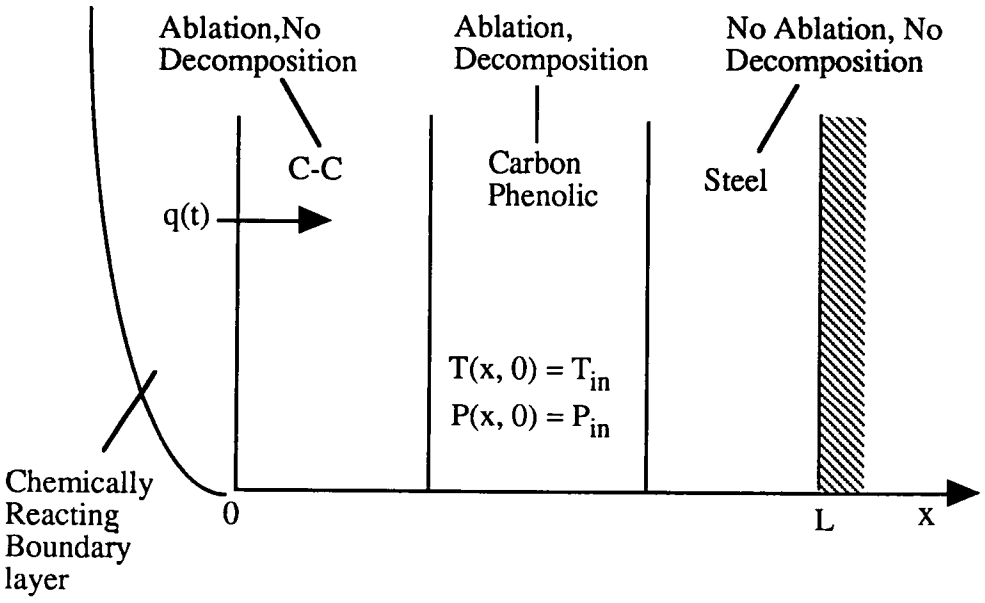

Fig 5.17 Description of test problem three

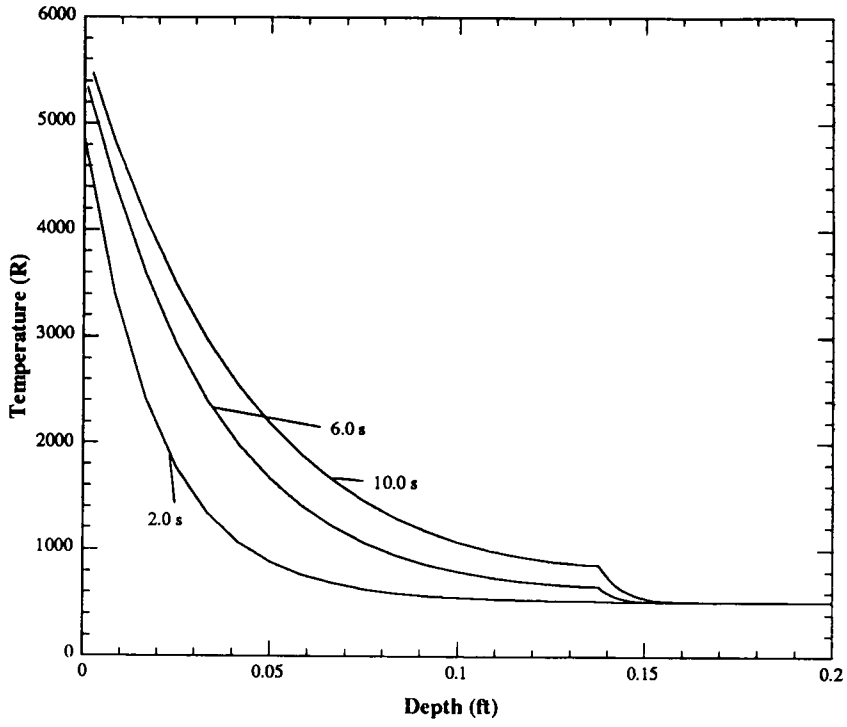

Fig 5.18 Temperature profiles in the domain

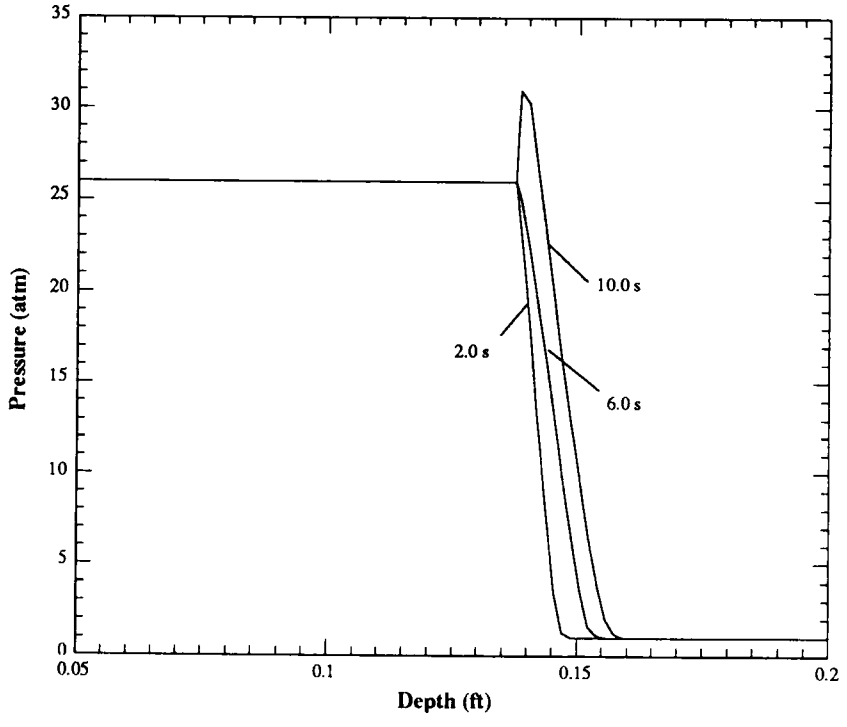

Fig 5.19 Pressure profiles in the domain

5.4 Test Case Four

This sample problem (fig. 5.20) shows that recession rate can be independently specified. A specified recession rate is given to show the efficiency of the ablation routine of the present model. Figures 5.21-5.22 show the development of temperature and pressure profiles in the material at times 2, 4, 6, 8 and 10 seconds. The input data for this problem is provided in the appendix A.

The material is subjected to a constant recession rate of 0.001 ft/s. The boundary at which this recession rate is imposed is held at a constant temperature and pressure. The back face of the domain is insulated and impermeable.

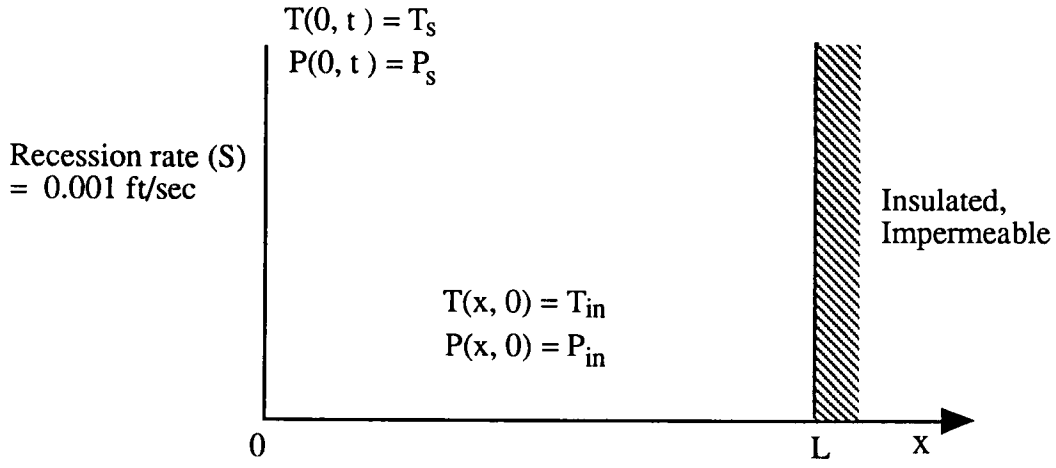

Fig 5.20 Description of the test problem four

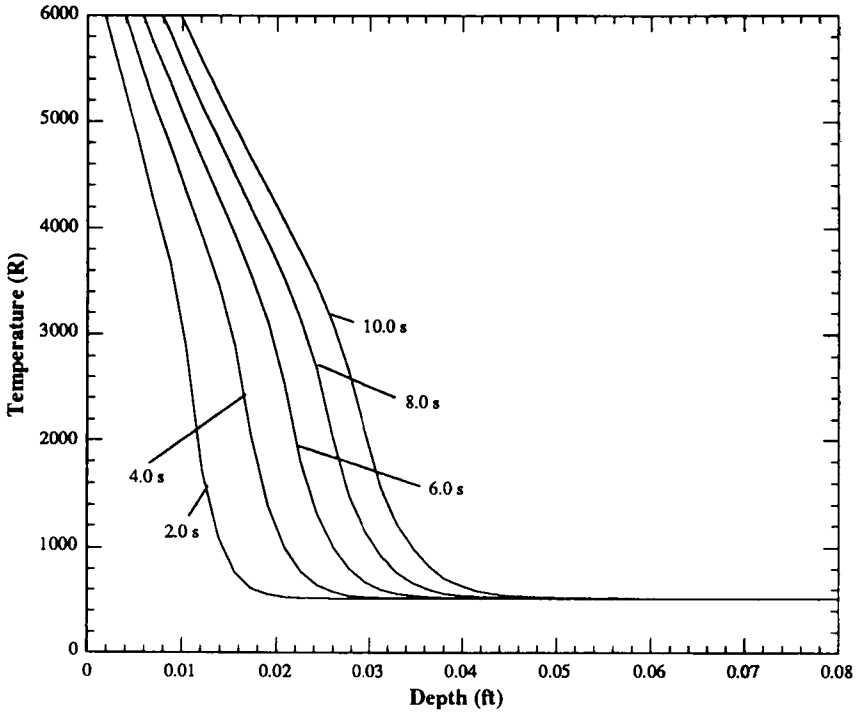

Fig 5.21 Temperature profiles in the domain

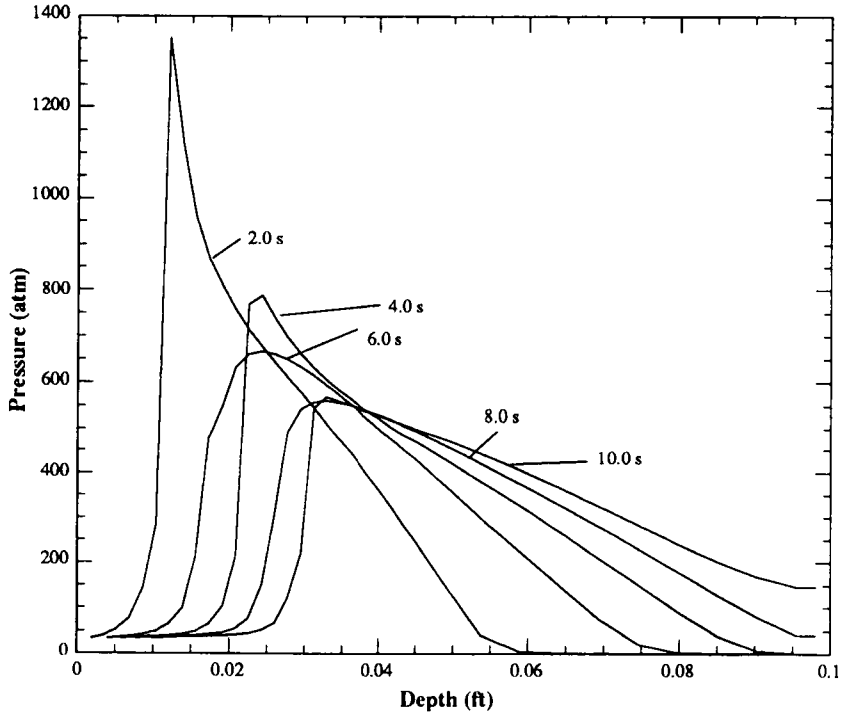

Fig 5.22 Pressure profiles in the domain

5.5 Test Case Five

This sample problem (fig. 5.23) is given to demonstrate the use of the general boundary condition Eq. (3.1) . The model as described earlier is capable of handling constant heat flux, radiative heating, convective and constant temperature boundary conditions independently. This sample problem gives an example of a constant boundary heat flux input at x = 0, and constant pressure boundary conditions on faces at x=0 and x=L. The boundary at x=L is kept insulated. Figures 5.24-5.25 show the development of the temperature and pressure profiles for 2, 4, 6, 8 and 10 seconds. The input data for this problem is provided in the appendix A.

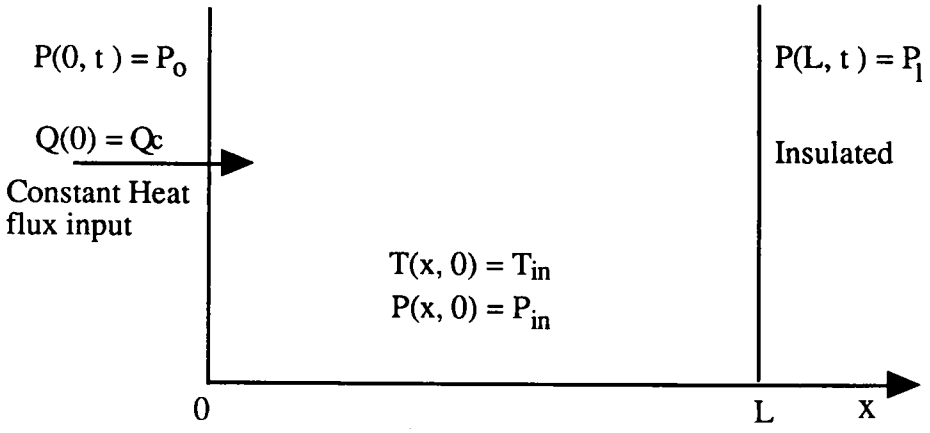

Fig 5.23 Description of the test problem five

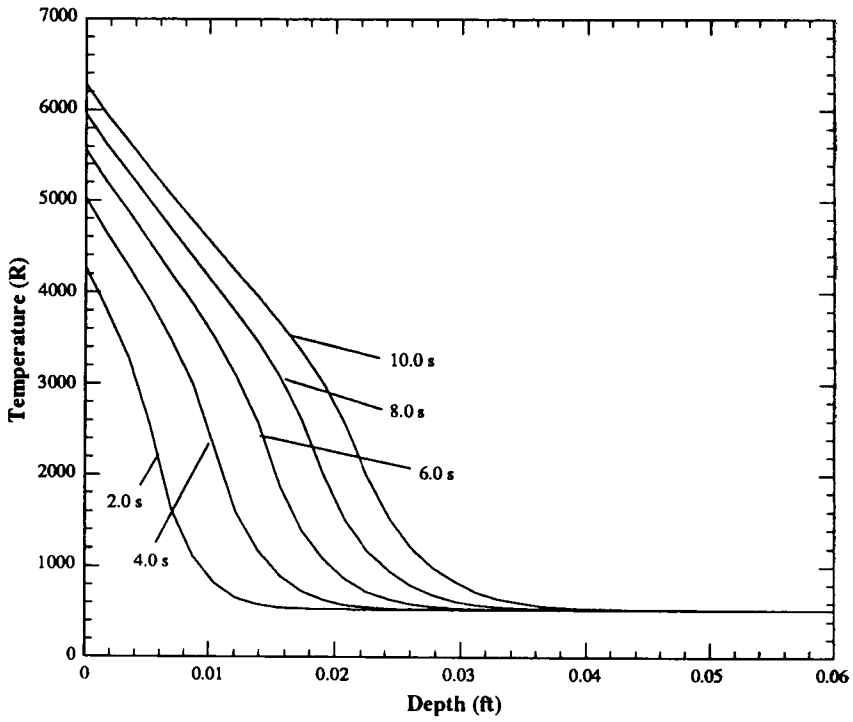

Fig 5.24 Temperature profiles in the domain

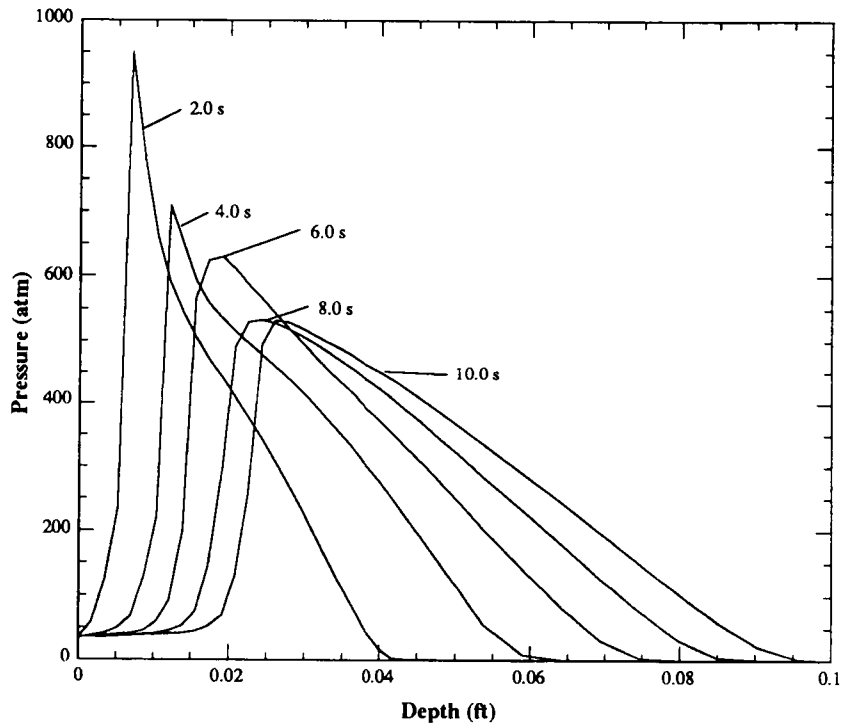

Fig 5.25 Pressure profiles in the domain

CONCLUSIONS

1) The pore pressure results of this work are based on the modified harmonic mean concept with upstream gas density (scheme d). Selection of the best scheme should be based on further studies and comparisons with closed form solutions, where possible. Work in progress by Polehn [21] may determine the appropriate procedure.

2) Generation of the Surface Heat Flux Tables is an efficient and time saving operation, and clearly shows that the Newton-Raphson iterative technique should be based on surface temperature as the independent variable. It should be noted that CMA uses the mass flow rate of char injected to the boundary ($\dot{m}_c$) as the independent variable in its surface iteration scheme.

3) Surface temperature oscillations may occur if one is using harmonic mean concept for evaluation of the effective thermal conductivity between two adjacent nodes. The present model uses the average temperature between two adjacent nodes to calculate virgin and char thermal conductivities, and the virgin volume fraction at the control volume face (x factor) to obtain the effective thermal conductivity. This approach does not result in oscillations in the predicted surface temperature.

4) An efficient numerical routine for tracking the surface is proposed as an alternative to the solution of governing equations based on a moving coordinate. This scheme is superior since it does not require reindexing of the variables and

dropping of the control volumes at the back face of the receding material. Therfore it can be easily implemented in a two dimensional model.

5) The CPU times for Test Case 2 on the VAX mainframe (8800s, VAX 2) of the University of Tennessee, Knoxville vaxcluster were recorded. This problem was solved with a time step of 0.008 seconds upto a time of 2.0 seconds (250 timesteps). The CMA (Charring Material Ablation) code used 246 timesteps to solve this problem. It should be noted that it is not possible to run CMA with a specified time step. The present model used 20.56 seconds of CPU time, while CMA required 66.72 seconds of CPU time. This difference should not be expected to hold for all problems. Another study performed for Marshall Space Flight Center showed that the present model is more than two times faster than CMA. This problem had sixteen time dependent entries for the surface thermochemistry table.

REFERENCES

REFERENCES

1) Bamford, C. H., Crank, J., and Malan, D. H., 1946, " The Combustion of Wood Part 1," *Cambridge Phil. Soc Proc.*, Vol 42., pp. 166 - 182.

2) Beavers, G. S., and Sparrow, E. M., 1971, " Compressible Gas Flow Through a Porous Material, " *Intl . Journal .Heat Mass Transfer,* Vol 14, pp. 1855 - 1859.

3) Blackshear, P. L., and Murty, K. A.,1965, " Heat and Mass Transfer to ,from, and Within Cellulosic Solids Burning in Air," *Tenth Symposium (International) on Combustion*, pp. 911 - 923.

4) Bruce, G. H., Peaceman, D. W., Rachford, H. H., and Rice, J. D., 1953, "Calculations of Unsteady-State Gas Flow through Porous Media," *Petroleum Transactions, AIME*, Vol 198, pp. 79 - 92.

5) Burke, S.P and Plummer, W.B., 1928, " Gas Flow Through Packed Columns," *Industrial Engineering Chemistry*, Vol 20, pp 1196-1200.

6) Ergun, S. and Orning, A.A., 1949, " Fluid Flow Through Randomly Packed Columns and Fluidized beds," *Industrial Engineering Chemistry,* Vol 11, pp 1179-1184.

7) Ergun, S., 1952, "Fluid flow through Packed Columns," *Chemical Engineering Progress*, Vol 48, pp 89-94.

8) Florio, J. Jr., 1989, "An Analytical and Experimental Investigation of the Decomposition of Glass Filled Polymer Composites," *Ph.D. Dissertation*, University of Rhode Island, Kingston, Rhode Island.

9) Florio, J. Jr., Henderson, J. B., Test, F. L., and Hariharan, R., 1991, " A Study of the Effects of the Assumption of Local - Thermal Equilibirium on the Overall

Thermally - Induced Response of a Decomposing, Glass - Filled Polymer Composite," *Intl . Journal Heat Mass Transfer*, Vol 34, pp. 135 - 147.

10) Forcheimer, Ph., 1901, "Wasserbewegung durch Bodan ," Zeitschriftdes Vereines Deutcher Ingenieure, Vol 45, pp 1781-1788.

11) Green, L. Jr. and Duwez, P., 1951, " Fluid Flow Through Porous Metals," *Journal of Applied Mechanics*, Vol 18, TRANS ASME, Vol73, Series E, pp 39-45.

12) Henderson, J. B., Wiebelt, J. A., and Tant, M. R., 1985," A Model for Thermal Response of Polymer Composite Material and Experimental Verification, "*Journal of Composite Material,* Vol 19, pp. 579 - 595.

13) Henderson, J. B., and Wiecek, T. E., 1987, " A Mathematical Model to Predict the Thermal Response of Decomposing, Expanding Polymer Composites ," *Journal of Composite Materials*, Vol 21, pp. 373 - 393.

14) Henderson, J. B., and Wiecek, T. E., 1988, " A Numerical Study of the Thermally Induced Respose of Decomposing, Expanding Composites, "*Warme und Stoffurbertragung* , Vol 22, pp. 275 - 284.

15) Keyhani, M., and Krishnan, V., 1992, " A One Dimensional Model for the Thermal Response of a Decomposing Polymer," AMD-Vol. 136, Computational Mechanics of Porous Materials and their Thermal Decomposition, ASME 1992.

16) Kung, H. C., 1972, "A Mathematical Model of Wood Pyrolysis," *Combustion and Flame* , Vol. 18, pp. 185 - 195.

17) Morrison, F. A. Jr.,1972," Transient Gas Flow in a Porous Column," *Industrial Engineering Chemistry Fundamentals* ,Vol 11, No. 2, pp. 191 - 197.

18) Patankar, S. V.,1980, *Numerical Heat Transfer and Fluid Flow*, Hemisphere Publishing Corporation. New York.

19) Panton, R. L., and Rittmann, J. G.,1971, " Pyrolysis of a Slab of Porous Material,"*Thirteenth Symposium (International) on Combustion*, pp. 881 - 891

20) Polbarinova-Kochina, P. Ya., 1962.,"Theory of Ground Water Movement," Princeton University Press, Princeton, New Jersey.

21) Polehn, R., " Thermal Response of an Axisymmetric Charring Decomposing Polymer," PhD dissertation in progress.

22) Moyer, C. B., and Rindal, R., 1963, "An Analysis of the Coupled Chemically Reacting Boundary Layer and Charring Ablator," *NASA contractor report NASA CR 1061.*

23) Ramamurthy, H., 1988," An Experimental Investigation into the Thermophysical Properties of Decomposing Polymer Composites," *M.S. Thesis*, University of Rhode Island, Kingston, Rhode Island.

24) Tinney, R. E., 1965, " The Combustion of Wooden Dowels in Heated Air," *Tenth Symposium (International) on Combustion*, pp. 925 - 930.

25) Shigenao, M., Aihara, T., and Viskanta, R., 1991, " Transient Behaviour of an Active Thermal Protection System," *Intl. Journal .Heat Mass Transfer,* Vol 34, No. 3, pp. 625 - 632.

26) Sullivan, R. M.,1989," A Finite Element Model for Thermally Decomposing Polymers," *Ph.D. Dissertation* , Pennsylvania State University.

27) Acurex final report FR - 84 -21/A TD , 1984, IUS Nozzle Material Thermal Characterization.

28) User's Manual, NonProprietary, Aerotherm Charring Material Thermal Response and Ablation Program. CMA87s., Acurex UM 87-13-ATD.

APPENDICES

APPENDIX A

Input Files for Test Cases

```
SAMPLE PROBLEM1, CONSTANT TEMPR BOUNDARY CONDITION
NO RECESSION RATE
 1 0 1  11 1                IFLAGP,ICHEM,MAINITRN,NODLET,NMBMAT
 1                          MATERIAL FLAGS(1-DECOMP,0-NODECOMP)
 5  0.01  0                 IPITER,TOLP,IFORCH
 10  0.675  0.0  0  0.0     TOL_SRF,CMBYCH,BREX,FLAGSDOT,SDOT
 1000.0  8314.4  5.67E-8     RADINR,UNIV_GASC,BOLTZ_CONST
 300.0  300.0               TREF1,TREF2
-0.025   2.0    0.2         ***TIMESTEPS**(DTIME,TTIME,PRTIME)
 0    0                     IPDETAIL,NDTIME
MATERIAL DATA -- ONE
 0.4  -9.0E+5  0.0   Resin Frac, Virgin Enthalpy,Char Enthalpy
 245.0   0.0    20.0     2.0    4600.0       310.0
 0.001   0.0    0.1E1    1.0    1.0         9000.0
 2230.0  1900.0  9.0E+10  3.0    19300.0      560.0
 300    1600.0 1.5  1.0  1.0  Temp,Cpvirgin,Kvirgin,Eps,Absrb
-3000.0 2500.0  8.0  1.0  1.0
 300.0  1600.0 1.5  1.0  1.0  Temp,Cpvirgin,Kvirgin,Eps,Absrb
-3000.0 2500.0  8.0  1.0  1.0
PYROLYSIS GAS TABLES
      300     -3.7e+6    Temp, Gas Enthalpy
   -3000       2.33E+7
PROPERTIES FOR PRESSURE CALC
    0.00    0.01    5E-20  Degree of Char, Porosity, Permeability
      0.25    0.095  3E-18
    0.50    0.18    3E-17
    0.75    0.265   2E-16
   -1.00    0.35        1E-13
      300     1.7E-5     17.0  Temp,Gas viscosity,Molecular Weight
   -3000      8.0E-5     11.0
NODAL DATA
   1     1    0.0005   Node Num, Mat ID, DX(NODE)
   2     1    0.0005
   3     1    0.0005
   4     1    0.0005
   5     1    0.0005
   6     1    0.0005
   7     1    0.0005
   8     1    0.0005
   9     1    0.0005
  10     1    0.0005
  11     1    0.0005
  12     1    0.0005
  13     1    0.0005
  14     1    0.0005
  15     1    0.0005
  16     1    0.0005
  17     1    0.0005
  18     1    0.0005
  19     1    0.0005
  20     1    0.0005
 -21     1   0.0
```

```
TEMP INITIAL AND BOUNDRY CONDITION
  300.0                        Initial temp
  0.0  0.0   5E30  0.0  3000 1)Epsg,Tsur,Ht Coeff,QFlux,Tambient
  0.0  0.0   0.0   0.0  0.0   2)Epsg,Tsur,Ht Coeff,QFlux,Tambient
PRES INITIAL AND BOUNDRY CONDITION
  101325.0                     Initial pres
  0.0  5E20  101325.0             1)Masfluxinp, Pres coeff, Pambient
  0.0  0.0   101325.0             2)Masfluxinp, Pres coeff, Pambient
```

SAMPLE PROBLEM2, (THERMOCHEM TABLES), NO FORCHEIMER TERM, SIMILAR TO CMASAMPLE2

```
 1 1 1 11 1                  IFLAGP,ICHEM,MAINITRN,NODLET,NMBMAT
 1                           MATERIAL FLAGS(1-DECOMP,0-NODECOMP)
 5 0.01  0                   IPITER,TOLP,FLGFORCH
 10 0.675 0.0 0 0.0          TOL_SRF,CMBYCH,FLGSDOT,SDOT
 2.244167  1545.35 4.76E-13   RADINR,UNIV_GASC,BOLTZ_CONST
 530.0  530.0                 TREF1,TREF2
 0.01  0.5  0.05             ***TIMESTEPS**(DTIME,TTIME,PRTIME)
 0.02  1.00  0.1             ***TIMESTEPS**(DTIME,TTIME,PRTIME)
 0.05  5.00  0.25             ***TIMESTEPS**(DTIME,TTIME,PRTIME)
-0.1  10.00  0.5             ***TIMESTEPS**(DTIME,TTIME,PRTIME)
 0   0                       IPDETAIL,NDTIME
MATERIAL DATA ONE
 0.401 -391.2  0.0 Resin Frac, Virgin enthalpy,Char Enthalpy
 15.48   0.0    0.2171E2   1.92   0.8329E+4   536
 0.001   0.0    0.1E1      1.0    1.0         9000
 139.2   118.9  0.9535E11  3.1    0.348E+5    1009
 530   0.41  0.264E-3  0.85  0.85 Temp,Cpvirgin,Kvirgin,Eps,Absrb
 800   0.41  0.292E-3  0.85  0.85
 1000  0.41  0.319E-3  0.85  0.85
 1200  0.41  0.322E-3  0.85  0.85
 1500  0.41  0.322E-3  0.85  0.85
 2000  0.41  0.322E-3  0.85  0.85
 2500  0.41  0.322E-3  0.85  0.85
 3000  0.493 0.322E-3  0.85  0.85
 3500  0.496 0.322E-3  0.85  0.85
 4000  0.498 0.322E-3  0.85  0.85
 5000  0.50  0.322E-3  0.85  0.85
-6000  0.50  0.322E-3  0.85  0.85
 530   0.41  0.322E-3  0.85  0.85 Temp,Cpchar,Kchar,Eps,Absrb
 800   0.41  0.322E-3  0.85  0.85
 1000  0.41  0.322E-3  0.85  0.85
 1200  0.41  0.322E-3  0.85  0.85
 1500  0.41  0.322E-3  0.85  0.85
 2000  0.41  0.400E-3  0.85  0.85
 2500  0.41  0.620E-3  0.85  0.85
 3000  0.493 0.104E-2  0.85  0.85
 3500  0.496 0.148E-2  0.85  0.85
 4000  0.498 0.190E-2  0.85  0.85
 4500  0.498 0.209E-2  0.85  0.85
 5000  0.50  0.228E-2  0.85  0.85
 5500  0.50  0.239E-2  0.85  0.85
-6000  0.50  0.25E-2   0.85  0.85
GAS ENTHALPY TABLES
      530    -1574.2   Temp, Gas Enthalpy
      1000   -1175.4
      1500   -665.1
      2000   -66.0
      2160   151.0
      2500   470.0
      3000   880.0
```

```
      3500   1260.0
      4050   1711.7
      4500   2165.1
      4950   2701.7
      5400   3415.3
      5850   4379.2
      6300   5698.5
      6750   7462.8
    -7300    9717.4
PROPERTIES FOR PRESSURE CALC
    0.00   0.005    3.0769E-19  Degree of Char,Porosity,Permeability
    0.294   0.016   2.2747E-18
    0.558   0.0477  1.3711E-17
    0.753   0.0898  5.1706E-17
     0.916    0.1614  5.75705E-15
    -1.00   0.35       1.0E-12
      500    0.33665E-6 17.0   Temp,Gas Viscosity,Molecular weight
      720    4.127E-7   17.36
      2880   9.988E-7   8.923
      3600   1.151E-6   8.643
      4320   1.299E-6   8.697
      5040   1.45E-6    9.18
      5760   1.618E-6   10.85
    -6500    0.1713E-5  12.65
NODAL DATA
    1    1   8.6666e-4   Node Number, Mat ID, DX(NODE)
    2    1   1.7333e-3
    3    1   1.7333e-3
    4    1   1.7333e-3
    5    1   1.7333e-3
    6    1   1.7333e-3
    7    1   1.7333e-3
    8    1   1.7333e-3
    9    1   1.7333e-3
   10    1   1.7333e-3
   11    1   1.7333e-3
   12    1   1.7333e-3
   13    1   1.7333e-3
   14    1   1.7333e-3
   15    1   1.7333e-3
   16    1   1.7333e-3
   17    1   1.7333e-3
   18    1   1.7333e-3
   19    1   1.7333e-3
   20    1   1.7333e-3
   21    1   1.7333e-3
   22    1   1.7333e-3
   23    1   1.7333e-3
   24    1   1.7333e-3
   25    1   1.7333e-3
   26    1   1.7333e-3
   27    1   1.7333e-3
```

```
   28    1    1.7333e-3
   29    1    1.7333e-3
   30    1    1.7333e-3
   31    1    5.2083e-3
   32    1    5.2083e-3
   33    1    5.2083e-3
   34    1    5.2083e-3
   35    1    5.2083e-3
   36    1    5.2083e-3
   37    1    5.2083e-3
   38    1    5.2083e-3
   39    1    5.2083e-3
  -40    1    0.0
 TEMP INITIAL AND BOUNDRY CONDITION
   520.0                Initial Temp
   0.0 0.0  0.0 0.0 0.0 Epsg,Tsur,Ht coeff,Qflux,Tambient
 PRESS INITIAL AND BOUNDRY CONDITION
   2116.8               Initial pressure
   0.0 0.0  0.0         MasFluxInp,Pres coeff,Pabient
 TIME DEPENDENT BOUNDRY CONDITIONS
   1.0                            Shape factor
  0.0 1137.00  650.36  0.884  34.23  0.4   Hr,Qradin,Htcoeff,Pr,BlwgP
 -30.0 1137.00  650.36  0.884  34.23  0.4   Hr,Qradin,Htcoeff,Pr,BlwgP
 SURFACE THERMOCHEMISTY TABLES
 1              Iconvert
34.2301 0.00000 0.000004000.00000.667 1675.023  829.225-1  CHAR    0.000E+00
34.2301 0.00000 0.000003500.00000.667 1323.840  580.077-1  CHAR    0.000E+00
34.2301 0.00000 0.000003000.00000.667  979.157  334.841-1  CHAR    0.000E+00
34.2301 0.00000 0.000002500.00000.667  644.290   95.899-1  CHAR    0.000E+00
34.2301 0.00000 0.000002000.00000.667  321.639 -134.904-1  CHAR    0.000E+00
34.2301 0.00000 0.000001500.00000.667   11.608 -357.171-1  CHAR    0.000E+00
34.2301 0.00000 0.000001000.00000.667 -284.598 -569.713-1  CHAR    0.000E+00
34.2301 0.00000 0.00000 500.00000.667 -560.945 -766.587-1  CHAR    0.000E+00
34.2301 0.50000 0.500003426.89640.667 2766.049 1887.898 1  C*      0.000E+00
34.2301 0.50000 0.200003052.43240.667 1796.524  999.509 1  C*      0.000E+00
34.2301 0.50000 0.175002982.68940.667 1665.996  893.414 1  C*      0.000E+00
34.2301 0.50000 0.125002777.46800.667 1343.066  642.383 1  C*      0.000E+00
34.2301 0.50000 0.100002603.22500.667 1121.629  478.195 1  C*      0.000E+00
34.2301 0.50000 0.025001221.77970.667 -377.435 -597.009 1  C*      0.000E+00
34.2301 0.50000 0.062501366.09680.667  -63.918 -342.261 1  C*      0.000E+00
34.2301 0.50000 0.081252373.07530.667  877.228  303.433 1  C*      0.000E+00
34.2301 0.50000 0.071882119.42810.667  645.901  143.890 1  C*      0.000E+00
34.2301 0.50000 0.067191417.44360.667   10.753 -286.119 1  C*      0.000E+00
34.2301 0.50000 0.069531472.08250.667   77.759 -237.745 1  C*      0.000E+00
34.2301 0.50000 0.070702054.16190.667  590.149  106.205 1  C*      0.000E+00
34.2301 0.50000 0.070122009.11530.667  552.224   80.715 1  C*      0.000E+00
34.2301 0.50000 0.069821979.78210.667  527.716   64.300 1  C*      0.000E+00
34.2301 0.50000 0.069681961.86150.667  512.803   54.332 1  C*      0.000E+00
34.2301 0.50000 0.010001186.67330.667 -481.762 -684.931 1  C*      0.000E+00
34.2301 0.50000 0.002001168.78890.667 -538.237 -732.587 1  C*      0.000E+00
34.2301 0.50000 0.001001166.55900.667 -545.401 -738.627 1  C*      0.000E+00
34.2301 0.50000 0.001001000.00000.667-1017.357-1115.059 0  CHAR    0.000E+00
```

34.2301 0.50000 0.00100 500.00000.667-1645.890-1595.500 0 CHAR 0.000E+00
34.2301 0.20000 0.500003511.05360.667 2774.065 1991.800 1 C* 0.000E+00
34.2301 0.20000 0.200003105.53490.667 1661.246 954.558 1 C* 0.000E+00
34.2301 0.20000 0.175003019.89450.667 1502.745 825.019 1 C* 0.000E+00
34.2301 0.20000 0.125002733.03690.667 1088.564 504.325 1 C* 0.000E+00
34.2301 0.20000 0.100002401.65150.667 746.773 254.224 1 C* 0.000E+00
34.2301 0.20000 0.025001147.23030.667 -595.498 -751.826 1 C* 0.000E+00
34.2301 0.20000 0.062501258.98660.667 -300.971 -502.176 1 C* 0.000E+00
34.2301 0.20000 0.081251361.08550.667 -119.308 -354.337 1 C* 0.000E+00
34.2301 0.20000 0.090632042.41630.667 455.122 49.487 1 C* 0.000E+00
34.2301 0.20000 0.085941419.64180.667 -44.598 -297.130 1 C* 0.000E+00
34.2301 0.20000 0.088281482.16110.667 21.131 -248.917 1 C* 0.000E+00
34.2301 0.20000 0.089451874.86580.667 330.890 -35.628 1 C* 0.000E+00
34.2301 0.20000 0.010001102.38390.667 -729.348 -864.109 1 C* 0.000E+00
34.2301 0.20000 0.002001072.65240.667 -816.304 -935.672 1 C* 0.000E+00
34.2301 0.20000 0.001001068.26360.667 -828.818 -945.855 1 C* 0.000E+00
34.2301 0.20000 0.001001000.00000.667 -997.085-1077.638 0 CHAR 0.000E+00
34.2301 0.20000 0.00100 500.00000.667-1591.202-1519.565 0 CHAR 0.000E+00
34.2301 0.10000 0.500003545.28430.667 2780.320 2038.272 1 C* 0.000E+00
34.2301 0.10000 0.200003128.68780.667 1609.400 939.363 1 C* 0.000E+00
34.2301 0.10000 0.175003036.10300.667 1438.846 799.546 1 C* 0.000E+00
34.2301 0.10000 0.125002704.94010.667 981.047 445.445 1 C* 0.000E+00
34.2301 0.10000 0.100002210.69760.667 531.807 118.858 1 C* 0.000E+00
34.2301 0.10000 0.025001110.55110.667 -692.239 -821.378 1 C* 0.000E+00
34.2301 0.10000 0.062501227.36410.667 -377.781 -554.280 1 C* 0.000E+00
34.2301 0.10000 0.081251309.13180.667 -214.301 -417.422 1 C* 0.000E+00
34.2301 0.10000 0.090631390.14490.667 -99.783 -326.299 1 C* 0.000E+00
34.2301 0.10000 0.095311515.68730.667 25.225 -233.616 1 C* 0.000E+00
34.2301 0.10000 0.097662068.12620.667 425.937 44.445 1 C* 0.000E+00
34.2301 0.10000 0.096481930.36220.667 327.940 -23.670 1 C* 0.000E+00
34.2301 0.10000 0.010001045.77490.667 -870.496 -967.573 1 C* 0.000E+00
34.2301 0.10000 0.00100 500.00000.667-1563.675-1482.425 0 CHAR 0.000E+00
34.2301 0.02500 0.500003573.69340.667 2786.930 2078.591 1 C* 0.000E+00
34.2301 0.02500 0.200003148.56800.667 1568.115 928.274 1 C* 0.000E+00
34.2301 0.02500 0.175003050.03990.667 1387.303 779.609 1 C* 0.000E+00
34.2301 0.02500 0.125002675.07160.667 889.655 394.879 1 C* 0.000E+00
34.2301 0.02500 0.100001501.86930.667 -7.610 -246.864 1 C* 0.000E+00
34.2301 0.02500 0.112502462.46140.667 688.236 246.263 1 C* 0.000E+00
34.2301 0.02500 0.106252273.92740.667 536.169 136.202 1 C* 0.000E+00
34.2301 0.02500 0.103132102.69630.667 411.388 47.308 1 C* 0.000E+00
34.2301 0.02500 0.101561922.73850.667 288.044 -39.395 1 C* 0.000E+00
34.2301 0.02500 0.025001071.34270.667 -786.287 -889.489 1 C* 0.000E+00
34.2301 0.02500 0.00100 614.22370.667-1472.814-1394.588 1 NH4CL* 0.000E+00
34.2301 0.02500 0.00100 500.00000.667-1536.158-1447.560 0 CHAR 0.000E+00
34.2301 0.01000 0.500003579.69920.667 2788.497 2087.310 1 C* 0.000E+00
34.2301 0.01000 0.200003152.84620.667 1559.608 926.115 1 C* 0.000E+00
34.2301 0.01000 0.175003053.04320.667 1376.601 775.544 1 C* 0.000E+00
34.2301 0.01000 0.125002667.81900.667 870.040 383.945 1 C* 0.000E+00
34.2301 0.01000 0.100001458.88130.667 -48.992 -275.012 1 C* 0.000E+00
34.2301 0.01000 0.112502442.62410.667 660.912 229.680 1 C* 0.000E+00
34.2301 0.01000 0.106252231.26840.667 495.166 109.854 1 C* 0.000E+00
34.2301 0.01000 0.103132005.18760.667 336.281 -2.944 1 C* 0.000E+00

34.2301 0.01000 0.101561547.00830.667 23.885 -221.978 1 C* 0.000E+00
34.2301 0.01000 0.025001060.84000.667 -809.940 -906.711 1 C* 0.000E+00
34.2301 0.01000 0.00200 615.35920.667-1464.544-1385.517 1 NH4CL* 0.000E+00
34.2301 0.01000 0.00100 615.97150.667-1465.221-1385.939 1 NH4CL* 0.000E+00
34.2301 0.01000 0.00100 500.00000.667-1528.009-1438.951 0 CHAR 0.000E+00
34.2301 0.00200 0.500003582.95000.667 2789.370 2092.057 1 C* 0.000E+00
34.2301 0.00200 0.200003155.17270.667 1555.037 924.974 1 C* 0.000E+00
34.2301 0.00200 0.175003054.67710.667 1370.839 773.365 1 C* 0.000E+00
34.2301 0.00200 0.125002663.73880.667 859.375 377.986 1 C* 0.000E+00
34.2301 0.00200 0.100001442.72470.667 -65.953 -286.464 1 C* 0.000E+00
34.2301 0.00200 0.112502431.13630.667 645.759 220.433 1 C* 0.000E+00
34.2301 0.00200 0.106252204.84930.667 471.103 94.251 1 C* 0.000E+00
34.2301 0.00200 0.103131920.49630.667 275.622 -44.148 1 C* 0.000E+00
34.2301 0.00200 0.025001054.64290.667 -823.614 -916.676 1 C* 0.000E+00
34.2301 0.00200 0.00200 616.32950.667-1460.336-1380.763 1 NH4CL* 0.000E+00
34.2301 0.00200 0.00100 616.97600.667-1460.943-1381.141 1 NH4CL* 0.000E+00
34.2301 0.00200 0.00100 500.00000.667-1523.210-1434.118 0 CHAR 0.000E+00
34.2301 0.00100 0.500003583.35870.667 2789.481 2092.656 1 C* 0.000E+00
34.2301 0.00100 0.200003155.46580.667 1554.464 924.832 1 C* 0.000E+00
34.2301 0.00100 0.175003054.88300.667 1370.116 773.093 1 C* 0.000E+00
34.2301 0.00100 0.125002663.21780.667 858.032 377.235 1 C* 0.000E+00
34.2301 0.00100 0.100001440.89840.667 -67.925 -287.792 1 C* 0.000E+00
34.2301 0.00100 0.112502429.65450.667 643.836 219.257 1 C* 0.000E+00
34.2301 0.00100 0.106252201.32500.667 467.963 92.207 1 C* 0.000E+00
34.2301 0.00100 0.103131905.93530.667 265.501 -51.071 1 C* 0.000E+00
34.2301 0.00100 0.025001053.82090.667 -825.413 -917.990 1 C* 0.000E+00
34.2301 0.00100 0.00100 617.10530.667-1460.396-1380.531 1 NH4CL* 0.000E+00
-34.2301 0.00100 0.00100 500.00000.667-1522.599-1433.506 0 CHAR 0.000E+00

SAMPLE PROBLEM3 (THERMOCHEM TABLES), MULTI MATERIAL, SIMILAR TO CMA SAMPLE3 PROBLEM

```
 1 1 1 11 3                    IFLAGP,ICHEM,MAINITRN,NODLET,NMBMAT
 1 1 0                         MATERIAL FLAG(1-DECOMP,0-NODECOMP)
 5 0.01 0                      IPITER,TOLP,FLGFORCH
 10 0.675 0.0 0 0.0            TOL_SRF,CMBYCH,FLGSDOT,SDOT
 2.244167 1545.35 4.76E-13     RADINR,UNIV_GASC,BOLTZ_CONST
 530.0 530.0                   TREF1,TREF2
 -0.05 10.00 2.00              ***TIMESTEPS**(DTIME,TTIME,PRTIME)
 0 0                           IPDETAIL,NDTIME
MATERIAL DATA ONE
 0.00 0.0 0.0 Resin Frac, Virgin Enthalpy, Char Enthalpy
 1.0 1.0 0.0 0.0 0.0 9000
 0.001 0.00 0.0 0.0 0.0 9000
 115.45 115.4 0.0 0.0 0.0 9000
 460 0.12 0.009024 0.8 0.8 Temp,Cpvirgin,Kvirgin,Eps,Absbr
-7000 0.57 0.004284 0.95 0.95
 460 0.12 0.009024 0.8 0.8 Temp,Cpchar,Kchar,Eps,Absbr
 960 0.32 0.007524 0.8 0.8
 1460 0.39 0.006828 0.79 0.79
 1960 0.44 0.005844 0.805 0.805
 2460 0.47 0.005088 0.82 0.82
 2960 0.49 0.004632 0.94 0.94
 3460 0.52 0.004404 0.94 0.94
 3960 0.54 0.004284 0.94 0.94
 4460 0.55 0.004284 0.94 0.94
 4960 0.55 0.004284 0.94 0.94
-7000 0.57 0.004284 0.95 0.95
GAS ENTHALPY TABLES
      530   -1574.2   Temp, Gas Enthalpy
      1000  -1175.4
      1500  -665.1
      2000  -66.0
      2160  151.0
      2500  470.0
      3000  880.0
      3500  1260.0
      4050  1711.7
      4500  2165.1
      4950  2701.7
      5400  3415.3
      5850  4379.2
      6300  5698.5
      6750  7462.8
  -7300     9717.4
PRESSURE CALC
   0.00  0.05  0.1E-13  Degree of Char,Porosity,Permeability
     -1.0  0.05  0.1E-13
     500   0.33665E-6 17.09  Temp,GAs Viscosity,Molecular weight
     720   4.127E-7  17.36
     1440  0.6581E-6  16.69
     2160  0.7683E-6  10.82
```

```
      2880   0.9988E-6  8.923
      3600   0.1151E-5  8.643
      4320   0.1299E-5  8.697
      5040   0.1450E-5  9.18
      5760   0.1618E-5  10.85
    -6500  0.1713E-5  12.610
MATERIAL TWO
 0.401 -391.2  0.0  Resin Frac,Virgin Enthalpy,Char enthalpy
 15.48   0.0    0.2171E2   1.92   0.8329E+4   536
 0.001   0.0    0.1E1      1.0    1.0         9000
 139.2   118.9  0.9535E11  3.1    0.348E+5    1009
 530.0 0.41  0.264E-3  Temp, Cpvirgin, Kvirgin
 800   0.41  0.292E-3
 1000  0.41  0.319E-3
 1200  0.41  0.322E-3
 1500  0.41  0.322E-3
 2000  0.41  0.322E-3
 2500  0.41  0.322E-3
 3000  0.493 0.322E-3
 3500  0.496 0.322E-3
 4000  0.498 0.322E-3
 5000  0.50  0.322E-3
-6000  0.50  0.311E-3
 530    0.41  0.322E-3  Temp,Cpchar, Kchar
 800   0.41  0.322E-3
 1000  0.41  0.322E-3
 1200  0.41  0.322E-3
 1500  0.41  0.322E-3
 2000  0.41  0.400E-3
 2500  0.41  0.620E-3
 3000  0.493 0.104E-2
 3500  0.496 0.148E-2
 4000  0.498 0.190E-2
 4500  0.498 0.209E-2
 5000  0.50  0.228E-2
 5500  0.50  0.239E-2
-6000  0.50  0.25E-2
GAS ENTHALPY TABLES
      530    -1574.2   Temp, Gas Enthalpy
      1000   -1175.4
      1500   -665.1
      2000   -66.0
      2160   151.0
      2500   470.0
      3000   880.0
      3500   1260.0
      4050   1711.7
      4500   2165.1
      4950   2701.7
      5400   3415.3
      5850   4379.2
      6300   5698.5
```

```
      6750   7462.8
    -7300     9717.4
PRESSURE CALC
    0.00   0.005    3.0769E-19  Degree of char, Porosity, Permeability
      0.294   0.016   2.2747E-18
    0.558   0.0477  1.3711E-17
    0.753   0.0898  5.1706E-17
      0.916   0.1614  5.75705E-15
   -1.00    0.35       1.0E-12
      500     0.33665E-6  17.0  Temp, Gas Viscosity, Molecular weight
      720     4.127E-7   17.36
      2880    9.988E-7   8.923
      3600    1.151E-6   8.643
      4320    1.299E-6   8.697
      5040    1.45E-6    9.18
      5760    1.618E-6   10.85
   -6500      0.1713E-5  12.65
MATERIAL THREE
  499.4                  Density
  400  0.107  0.00611  Temp,Cp,Thermal conductivity
  600  0.11   0.00681
  700  0.115  0.00694
  800  0.12   0.00688
  900  0.125  0.00678
 1000  0.13   0.0066
 1200  0.145  0.00625
 1400  0.16   0.00576
 1600  0.175  0.00528
 2000  0.165  0.00425
 3000  0.165  0.00425
 4000  0.165  0.00425
 5000  0.165  0.00425
-6000  0.165  0.00425
NODAL DATA
   1    1   4.16667e-3  Node num,Mat ID, DX(NODE)
   2    1   8.3333e-3
   3    1   8.3333e-3
   4    1   8.3333e-3
   5    1   8.3333e-3
   6    1   8.3333e-3
   7    1   8.3333e-3
   8    1   8.3333e-3
   9    1   8.3333e-3
  10    1   8.3333e-3
  11    1   8.3333e-3
  12    1   8.3333e-3
  13    1   8.3333e-3
  14    1   8.3333e-3
  15    1   8.3333e-3
  16    1   8.3333e-3
  17    1   8.3333e-3
  18    2   0.0
```

```
   19    2   1.7333e-3
   20    2   1.7333e-3
   21    2   1.7333e-3
   22    2   1.7333e-3
   23    2   1.7333e-3
   24    2   1.7333e-3
   25    2   1.7333e-3
   26    2   1.7333e-3
   27    2   1.7333e-3
   28    2   1.7333e-3
   29    2   1.7333e-3
   30    2   1.7333e-3
   31    2   1.7333e-3
   32    2   1.7333e-3
   33    2   1.7333e-3
   34    2   1.7333e-3
   35    2   1.7333e-3
   36    2   1.7333e-3
   37    2   1.7333e-3
   38    2   1.7333e-3
   39    2   1.7333e-3
   40    2   1.7333e-3
   41    2   1.7333e-3
   42    2   1.7333e-3
   43    2   1.7333e-3
   44    2   1.7333e-3
   45    2   1.7333e-3
   46    2   1.7333e-3
   47    2   5.2083e-3
   48    2   5.2083e-3
   49    2   5.2083e-3
   50    2   5.2083e-3
   51    2   5.2083e-3
   52    2   5.2083e-3
   53    2   5.2083e-3
   54    2   5.2083e-3
   55    2   5.2083e-3
   56    3   0.0
   57    3   0.039166
  -58    3   0.0
 TEMP INITIAL AND BOUNDRY CONDITION
   520.0                Initial Temp
   0.0 0.0   0.0 0.0 0.0   Epsg,Tsur,Ht coeff,Qflux,Tambient
 PRESS INITIAL AND BOUNDRY CONDITION
   2116.8               Initial Pressure
   0.0 0.0   0.0        MasFluxInp,Pres coeff, Pambient
 THERMOCHEMISTRY BOUNDRY CONDITIONS
   1.0                          Shape Factor
  -1e-20 1075.000  620.0   0.8029   26.0   0.4 Hr,Qradin,Ht coeff,Pr,Blwg
 SURFACE THERMOCHEMISTRY TABLES
 1              ICONVERT
26.0000 0.00000 0.000004000.00000.667 1715.933  820.014
```

26.0000 0.00000 0.000003500.00000.667 1370.880 576.213
26.0000 0.00000 0.000003000.00000.667 1031.432 335.735
26.0000 0.00000 0.000002500.00000.667 698.379   99.080
26.0000 0.00000 0.000002000.00000.667 376.559 -130.184
26.0000 0.00000 0.000001500.00000.667   70.083 -348.854
26.0000 0.00000 0.000001000.00000.667 -220.464 -556.225
26.0000 0.00000 0.00000 500.00000.667 -492.213 -748.797
26.0000 0.80290 0.703094000.00000.667 4030.254 2972.004
26.0000 0.80290 0.394453800.00000.667 3155.760 2093.450
26.0000 0.80290 0.228433600.00000.667 2371.897 1378.028
26.0000 0.80290 0.138053400.00000.667 1754.484 865.226
26.0000 0.80290 0.103773200.00000.667 1338.155 587.113
26.0000 0.80290 0.065083000.00000.667 954.353 355.373
26.0000 0.80290 0.036822800.00000.667 645.304 156.499
26.0000 0.80290 0.021162600.00000.667 410.391   -2.425
26.0000 0.80290 0.011922400.00000.667 219.281 -138.258
26.0000 0.80290 0.006282200.00000.667   54.515 -260.539
26.0000 0.80290 0.002962000.00000.667 -94.059 -374.315
26.0000 0.80290 0.001191800.00000.667 -231.435 -480.518
26.0000 0.80290 0.000381600.00000.667 -360.213 -579.342
26.0000 0.80290 0.000091400.00000.667 -485.273 -675.679
26.0000 0.80290 0.000011200.00000.667 -648.130 -802.811
26.0000 0.80290 0.000001000.00000.667-1023.835-1088.296
26.0000 0.80290 0.00000 500.00000.667-1595.037-1483.651
26.0000 0.00001 0.703094000.00000.667 4030.254 2972.004
26.0000 0.00001 0.394453800.00000.667 3155.760 2093.450
26.0000 0.00001 0.228433600.00000.667 2371.897 1378.028
26.0000 0.00001 0.138053400.00000.667 1754.484 865.226
26.0000 0.00001 0.103773200.00000.667 1338.155 587.113
26.0000 0.00001 0.065083000.00000.667 954.353 355.373
26.0000 0.00001 0.036822800.00000.667 645.304 156.499
26.0000 0.00001 0.021162600.00000.667 410.391   -2.425
26.0000 0.00001 0.011922400.00000.667 219.281 -138.258
26.0000 0.00001 0.006282200.00000.667   54.515 -260.539
26.0000 0.00001 0.002962000.00000.667 -94.059 -374.315
26.0000 0.00001 0.001191800.00000.667 -231.435 -480.518
26.0000 0.00001 0.000381600.00000.667 -360.213 -579.342
26.0000 0.00001 0.000091400.00000.667 -485.273 -675.679
26.0000 0.00001 0.000011200.00000.667 -648.130 -802.811
26.0000 0.00001 0.000001000.00000.667-1023.835-1088.296
-26.0000 0.00001 0.00000 500.00000.667-1595.037-1483.651

SAMPLE PROBLEM4, CONSTANT TEMPR AND PRESS B.C. CONSTANT RECESSION RATE AND VARIABLE TIME STEP

```
 1 0 1  11 1                IFLAGP,ICHEM,MAINITRN,NODLET,NMBMAT
 1                          MATERIAL FLAGS(1-DECOMP,0-NODECOMP)
 5 0.01  0                  IPITER,TOLP,FLGFORCH
 10 0.675 0.0 1 0.001       TOL_SRF,CMBYCH,BREX,FLGSDOT,SDOT
 10000 1545.35 4.76E-13     RADINR,UNIV_GASC,BOLTZ_CONST
 530.0  530.0               TREF1,TREF2
-0.2   10.00   5.0          ***TIMESTEPS**(DTIME,TTIME,PRTIME)
 1   5                      IPDETAIL,NDTIME
MATERIAL DATA -- ONE
 0.401 -391.2  0.0   Resin Frac,Virgin Enthalpy,Char Enthalpy
 15.48   0.0   0.2171E2   1.92   0.8329E+4   536
 0.001   0.0   0.1E1      1.0    1.0         9000
 139.2   118.9 0.9535E11  3.1    0.348E+5    1009
 530   0.41  0.264E-3  0.8 0.8  Temp,Cpvirgin,Kvirgin,Eps,Absrb
 800   0.41  0.292E-3  0.8 0.8
 1000  0.41  0.319E-3  0.8 0.8
 1200  0.41  0.322E-3  0.8 0.8
 1500  0.41  0.322E-3  0.8 0.8
 2000  0.41  0.322E-3  0.8 0.8
 2500  0.41  0.322E-3  0.8 0.8
 3000  0.493 0.322E-3  0.8 0.8
 3500  0.496 0.322E-3  0.8 0.8
 4000  0.498 0.322E-3  0.8 0.8
 5000  0.50  0.322E-3  0.8 0.8
-6000  0.50  0.322E-3  0.8 0.8
 530   0.41  0.322E-3  0.8 0.8  Temp,Cpchar,Kchar,Eps,Absrb
 800   0.41  0.322E-3  0.8 0.8
 1000  0.41  0.322E-3  0.8 0.8
 1200  0.41  0.322E-3  0.8 0.8
 1500  0.41  0.322E-3  0.8 0.8
 2000  0.41  0.400E-3  0.8 0.8
 2500  0.41  0.620E-3  0.8 0.8
 3000  0.493 0.104E-2  0.8 0.8
 3500  0.496 0.148E-2  0.8 0.8
 4000  0.498 0.190E-2  0.8 0.8
 4500  0.498 0.209E-2  0.8 0.8
 5000  0.50  0.228E-2  0.8 0.8
 5500  0.50  0.239E-2  0.8 0.8
-6000  0.50  0.25E-2   0.8 0.8
GAS ENTHALPY TABLES
      530    -1574.2  Temp,Gas Enthalpy
      1000   -1175.4
      1500   -665.1
      2000   -66.0
      2160   151.0
      2500   470.0
      3000   880.0
      3500   1260.0
      4050   1711.7
      4500   2165.1
```

```
      4950   2701.7
      5400   3415.3
      5850   4379.2
      6300   5698.5
      6750   7462.8
    -7300    9717.4
PROPERTIES FOR PRESSURE CALC
    0.00   0.005    3.0769E-19  Degree char,Porosity,Permeability
    0.294   0.016   2.2747E-18
    0.558   0.0477  1.3711E-17
    0.753   0.0898  5.1706E-17
     0.916   0.1614  5.75705E-15
    -1.00   0.35       1.0E-12
      500    0.33665E-6  17.0  Temp,Gas Viscosity, Molecular weight
      720    4.127E-7   17.36
      2880   9.988E-7   8.923
      3600   1.151E-6   8.643
      4320   1.299E-6   8.697
      5040   1.45E-6    9.18
      5760   1.618E-6   10.85
    -6500    0.1713E-5  12.65
NODAL DATA
    1    1   0.0        Node number, Mat ID, DX(node)
    2    1   1.7333e-3
    3    1   1.7333e-3
    4    1   1.7333e-3
    5    1   1.7333e-3
    6    1   1.7333e-3
    7    1   1.7333e-3
    8    1   1.7333e-3
    9    1   1.7333e-3
   10    1   1.7333e-3
   11    1   1.7333e-3
   12    1   1.7333e-3
   13    1   1.7333e-3
   14    1   1.7333e-3
   15    1   1.7333e-3
   16    1   1.7333e-3
   17    1   1.7333e-3
   18    1   1.7333e-3
   19    1   1.7333e-3
  -20    1   0.0
TEMP INITIAL AND BOUNDRY CONDITION
   520.0                              Initial temp
   0.0 0.0 5e30 0.0 6000.0            1)Epsg,Tsur,Ht Coeff,QFlux,Tambient
   0.0 0.0 0.0 0.0 00.0               2)Epsg,Tsur,Ht Coeff,QFlux,Tambient
PRESSURE INITIAL AND BOUNDRY CONDITION
   2116.8                         Initial pres
   0.0 5E20  72394.56             MasFluxInp, Pres coeff, Pambient
   0.0 0.0   0.0                  MasFluxInp, Pres coeff, Pambient
```

```
 SAMPLE PROBLEM5, CONSTANT HEAT FLUX BC, AND CONSTANT
 PRESS ON BOTH FACES, NO RECESSION, BACK FACE INSULATED
 1 0 1 11 1                IFLAGP,ICHEM,MAINITRN,NODLET,NMBMAT
 1                         MATERIAL FLAGS(1-DECOMP,0-NODECOMP)
 5 0.01 0                  IPITER,TOLP,FLGFORCH
 10 0.675 0.0 0 0.0        TOL_SRF,CMBYCH,BREX,FLGSDOT,SDOT
 2.244167 1545.35 4.76E-13     RADINR,UNIV_GASC,BOLTZ_CONST
 530.0 530.0                   TREF1,TREF2
-0.05   10.00  2.0              ***TIMESTEPS**(DTIME,TTIME,PRTIME)
 0    0                        IPDETAIL,NDTIME
MATERIAL DATA ONE
 0.401 -391.2  0.0    Resin Frac, Virgin Enthalpy, Char Enthalpy
 15.48   0.0   0.2171E2   1.92   0.8329E+4   536
 0.001   0.0   0.1E1      1.0    1.0         9000
 139.2   118.9  0.9535E11  3.1   0.348E+5    1009
 530   0.41  0.264E-3  0.8 0.8  Temp, Cpvirgin,Kvirgin,Eps,Absrb
 800   0.41  0.292E-3  0.8 0.8
 1000  0.41  0.319E-3  0.8 0.8
 1200  0.41  0.322E-3  0.8 0.8
 1500  0.41  0.322E-3  0.8 0.8
 2000  0.41  0.322E-3  0.8 0.8
 2500  0.41  0.322E-3  0.8 0.8
 3000  0.493 0.322E-3  0.8 0.8
 3500  0.496 0.322E-3  0.8 0.8
 4000  0.498 0.322E-3  0.8 0.8
 5000  0.50  0.322E-3  0.8 0.8
-6000  0.50  0.322E-3  0.8 0.8
 530   0.41  0.322E-3  0.8 0.8  Temp, Cpchar,Kchar,Eps,Absrb
 800   0.41  0.322E-3  0.8 0.8
 1000  0.41  0.322E-3  0.8 0.8
 1200  0.41  0.322E-3  0.8 0.8
 1500  0.41  0.322E-3  0.8 0.8
 2000  0.41  0.400E-3  0.8 0.8
 2500  0.41  0.620E-3  0.8 0.8
 3000  0.493 0.104E-2  0.8 0.8
 3500  0.496 0.148E-2  0.8 0.8
 4000  0.498 0.190E-2  0.8 0.8
 4500  0.498 0.209E-2  0.8 0.8
 5000  0.50  0.228E-2  0.8 0.8
 5500  0.50  0.239E-2  0.8 0.8
-6000  0.50  0.25E-2   0.8 0.8
GAS ENTHALPY TABLES
      530    -1574.2   Temp, Gas Enthalpy
      1000   -1175.4
      1500   -665.1
      2000   -66.0
      2160   151.0
      2500   470.0
      3000   880.0
      3500   1260.0
      4050   1711.7
      4500   2165.1
```

```
      4950   2701.7
      5400   3415.3
      5850   4379.2
      6300   5698.5
      6750   7462.8
    -7300    9717.4
PROPERTIES FOR PRESSURE CALC
    0.00   0.005    3.0769E-19 Degree of char,Porosity,Permeability
      0.294   0.016   2.2747E-18
    0.558   0.0477  1.3711E-17
    0.753   0.0898  5.1706E-17
      0.916   0.1614  5.75705E-15
    -1.00   0.35       1.0E-12
      500    0.33665E-6  17.0  Temp, Gas Viscosity, Molecular weight
      720    4.127E-7   17.36
      2880   9.988E-7   8.923
      3600   1.151E-6   8.643
      4320   1.299E-6   8.697
      5040   1.45E-6    9.18
      5760   1.618E-6   10.85
    -6500    0.1713E-5  12.65
NODAL DATA
    1    1   8.6666e-4  Node number,Mat ID, DX(NODE)
    2    1   1.7333e-3
    3    1   1.7333e-3
    4    1   1.7333e-3
    5    1   1.7333e-3
    6    1   1.7333e-3
    7    1   1.7333e-3
    8    1   1.7333e-3
    9    1   1.7333e-3
   10    1   1.7333e-3
   11    1   1.7333e-3
   12    1   1.7333e-3
   13    1   1.7333e-3
   14    1   1.7333e-3
   15    1   1.7333e-3
   16    1   1.7333e-3
   17    1   1.7333e-3
   18    1   1.7333e-3
   19    1   1.7333e-3
   20    1   1.7333e-3
   21    1   1.7333e-3
   22    1   1.7333e-3
   23    1   1.7333e-3
   24    1   1.7333e-3
   25    1   1.7333e-3
   26    1   1.7333e-3
   27    1   1.7333e-3
   28    1   1.7333e-3
   29    1   1.7333e-3
   30    1   1.7333e-3
```

```
  31    1    5.2083e-3
  32    1    5.2083e-3
  33    1    5.2083e-3
  34    1    5.2083e-3
  35    1    5.2083e-3
  36    1    5.2083e-3
  37    1    5.2083e-3
  38    1    5.2083e-3
  39    1    5.2083e-3
 -40    1    0.0
TEMP INITIAL AND BOUNDRY CONDITION
  520.0                          Initial Temp
  0.0 0.0  0.0 500.0 0.0   1)Epsg,Tsur,Ht Coeff,Qflux,Tambient
  0.0 0.0  0.0 0.0 0.0     2)Epsg,Tsur,Ht Coeff,Qflux,Tambient
PRESS INITIAL AND BOUNDRY CONDITION
  2116.8                         Initial pressure
  0.0 5E20  72394.56       1)MasFluxInp, Pres coeff, Pambient
  0.0 5E20   2116.8        2)MasFluxInp, Pres coeff, Pambient
```

APPENDIX B

User's Manual : Input File Format

User's Manual : Input File Format

The first two lines of the input file are dedicated to the *title* and *brief description* of the problem. These lines are echoed in the ouput information. The flag and data lines are inputted after the title lines as described below.

Line 1

1) Iflagp — Flag for invoking pressure solution
   = 1 - Pressure solution invoked (convection cooling invoked)
   = 0 - No pressure solution (no convection cooling effects)

2) Ichem — Thermochemistry table input flag
   = 1 - Thermochemistry table
   = 0 - No thermochemistry table Eq. (3.1) to be used for surface boundary condition

3) Mainitrn — Number of main Iterations
   = 1 - Weakly coupled
   > 1 - Fully coupled

4) Nodlet — Number of nodelets per control volume, must be an odd number. Minimum acceptable input value is 3.

5) Nmbmat — Number of materials in the computational domain

Line 2

1) Matid(k) — Material ID for kth material
   = 1 - Decomposing and/or porous material
   = 0 - Nondecomposing, non porous solid

Line 3

1) Ipiter — Number of iterations for pressure solution

2) Tolp — Tolerance for pressure solution

3) Flgforch — Flag for inertial (Forcheimer) coefficient.
   = 1 - Invoked
   = 0 - Not invoked

If Iflagp = 0, these values are not expected in the read routine. Instead data of line 4 is expected.

Line 4

1) Tol_srf	Tolerance for the surface temperature convergence (degrees)
2) Cmbych	C_M/C_H - Ratio of mass to heat transfer coefficients
3) Brex	Burning rate exponent
4) Flgsdot	Specified recession rate
	= 1 , Invoked
	= 0 , Not invoked
5) Sdot	Specified recession rate

Line 5

1) Radinr	Inner radius of the problem
2) Univ_gasc	Universal gas constant
3) Boltz_const	Stefan Boltzman constant

Line 6

1) Tref1	Reference temperature for enthalpy of formation of virgin material
2) Tref2	Reference temperature for enthalpy of formation of char material

Line 7

1) Dtime	Timestep for evaluation
2) Ttime	Final time for the above time step
3) Prtime	Print interval up to the above final time

Repeat as desired. Time data is read until negative Dtime is encountered.

Line 8

1) Ipdetail	Flag to print time, surface heat flux, surface temperature, recession rate, surface location, location of maximum pressure and maximum pressure in an output file named *input _file _name .plt.*
	= 1 -- Invoked
	= 0 -- Not invoked
2) Ndtime	Interval for printing data

MATERIAL DATA ONE ---- heading must be input

Line 1

1) Resin frac — Resin fraction
2) Virgin enthalpy — Enthalpy of formation of virgin material
3) Char enthalpy — Enthalpy of formation of char material

Lines 2-4

Decomposition kinetic data of components A, B and C

For a non-decomposing porous material, e.g., carbon-carbon composite, the following procedure should be used. For each component, the input virgin density should be equal to its char value. Furthermore, the input cutoff temperature for each component should be greater than the maximum expected temperature in the domain during the transient.

Next line(s)

Virgin properties : data read as,

Temp, Specific heat , Thermal conductivity, Emissivity, Absorbtivity

Read until negative Temp is encountered.

Char properties : Read similar to and immediately after virgin properties.

Data read till negative char temperature is encountered.

Emissivity and absorbtivity data are required for the first material only when Ichem = 1.

GAS ENTHALPY TABLES ---- heading must be input

Gas enthalpy : data read as,

1) Temp, Gas enthalpy

Read until negative temperature is encountered.

PROPERTIES FOR PRESSURE CALC ---- heading must be input

Read as:

Degree of char, Porosity, Permeability

Read until negative degree of char is encountered.

If inertia effect is considered then data is read as:

Degree of char, Porosity, Permeability, Forcheimer coefficient

Gas viscosity and molecular weight : data read as,
Temp, Gas viscosity, Molecular weight
Read until negative temperature is encountered.
When Iflagp = 0, the section on properties for the pressure calculation should be omitted.

MATERIAL DATA TWO ---- heading must be input (The following is an example for a solid non-decomposing material two)
Line 1 Density

Next line(s)
Properties data : for material 2 read as,
Temp, Specific heat, Thermal conductivity
Read until negative temperature is encountered.

Read depending upon the number of materials, e.g., If Nmbmat = 1, only one material is read.

NODAL DATA ---- heading must be input
Data read as :
Node number, Material number, Node size
If a number of materials are present, the interface between two materials is a zero control volume ($\Delta x = 0$), belonging to the next material.

TEMP INITIAL AND BOUNDARY CONDITION ---- heading must be input
Line 1 Initial Temperature

Next line(s)
Data read as :
1) Emissivity, Tsurrounding for radiation, Heat transfer coefficient for convection, Constant heat flux input, Ambient temperature for convection, and dT/dt for time rate of change in temperature applied to Tsurrounding and Ambient temperature for surface at x = 0 (when Ichem = 1, this data should not be inputted)

2) Emissivity, Tsurrounding for radiation, Heat transfer coefficient for convection, Constant heat flux input, Ambient temperature for convection, and dT/dt for time rate of

change in temperature applied to Tsurrounding and Ambient temperature for surface at x = L (This data should be inputted for any value of Ichem)

For a specified surface temperature simply set heat transfer coefficient to 1.0E+20, and the code will set the surface temperature equal to the ambient temperature (emissivity and heat flux must be set equal to zero).

PRES INITIAL AND BOUNDARY CONDITION ---- heading must be input

Line 1 Initial pressure

Next line(s)

Data read as :

1) Mass flux input, Convective mass transfer coefficient, Ambient pressure, and dP/dt for time rate of change in ambient pressure for surface at x = 0 (when Ichem = 1, this data should not be inputted)

2) Mass flux input, Convective mass transfer coefficient, Ambient pressure, and dP/dt for time rate of change in ambient pressure for surface at x = L (This data should be inputted for any value of Ichem)

For a specified surface pressure simply set convective mass transfer coefficient to 1.0E+20, and the code will set the surface pressure equal to the ambient pressure (mass flux input must be set equal to zero). The pressure initial and boundary condition information should be omitted when Iflagp = 0.

TIME DEPENDENT BOUNDARY CONDITION (when Ichem = 1)

--- heading must be input

Line 1 Shape factor

Line 2

Data read as : Time, Hedge, Qradinp, Rucho, Brep

Time = Time at which surface variables are evaluated

Hedge = Enthalpy of the edge gas

Qradinp = Radiation flux input

Rucho = Heat coefficient

Brep = Blowing reduction parameter

Read until negative time is encountered.

SURFACE THERMOCHEMISTRY TABLES --- heading must be input

Line 1

Iconvert = 1

Flag for a consistent set of units for the ACE thermochemistry table.

ACE thermochemistry table in units of meter, kg, second and calories should be inputted (as used in CMA). The code will convert to units of foot, lbm, second and Btu. The user should make sure that the rest of the input file is in units of foot, lbm, second and Btu.

Iconvert = 0

The units of the thermochemistry input data will not be converted. Therefore, the user must make sure that the entire input data are in consistent units with the thermochemistry input table.

Next lines

Thermochemistry tables in the same format as CMA

Read until negative pressure is encountered. End of input file. The section on thermochemistry tables should be omitted when Ichem=0.

The code can read the thermochemistry tables in the same format as CMA. The user can cut and paste a CMA thermochemistry table in this section of the input file.

Output and unit assignments

The output file echoes the input data in the same units as the user has used to create the input file. The pressure results are dimensionless values representing the ratio of pressure to the initial pressure value.

Batch job unit assignments:

Unit 9 for Input_file_name.inp

Unit 10 for Input_file_name.out

Unit 11 for Input_file_name.plt

Vita

Vikram Krishnan was born in Copenhagen, Denmark, on August 10, 1967. He attended elementary and secondary school at Kendriya Vidyalaya in Bangalore, India through tenth standard and received his secondary schhol certificate in 1982. He received his higher secondary school certificate in 1984. He represented his school in cricket.

In 1984, he enrolled in the National Institute of Engineering, Mysore, India. He represented his college in the intercollegiate cricket tournaments. In December 1988, he received a Bachelor in Engineering with a major in Mechanical Engineering. In the fall of 1990, the author enrolled in the master's degree program in Mechanical Engineering at the University of Tennessee, Knoxville, U.S.A. The degree was awarded in August 1992. The author has coauthored a few technical research papers. The field of his expertise is thermal sciences. The author wishes to pursue a teaching and research career in the general area of thermal sciences. The author is an associate member of the American Society of Mechanical Engineers.